CALSPAN
UB
RESEARCH CENTER

DTIC
S ELECTE
C MAY 6 1993 D

KINETICS OF NITRIC OXIDE FORMATION BEHIND 3 TO 4 KM/S SHOCK WAVES

Final Report

by Charles E. Treanor and Marcia J. Williams

February 15, 1993

Calspan-UB Research Center
P. O. Box 400
Buffalo, NY 14225

93-09744

'93 5 05 037

REPORT DOCUMENTATION PAGE

Form Approved
OMB No. 0704-0188

Public reporting burden for this collection of information is estimated to average 1 hour per response, including the time for reviewing instructions, searching existing data sources, gathering and maintaining the data needed, and completing and reviewing the collection of information. Send comments regarding this burden estimate or any other aspect of this collection of information, including suggestions for reducing this burden, to Washington Headquarters Service., Directorate for Information Operations and Reports, 1215 Jefferson Davis Highway, Suite 1204, Arlington, VA 22202-4302, and to the Office of Management and Budget, Paperwork Reduction Project (0704-0188), Washington, DC 20503.

1. AGENCY USE ONLY (Leave blank)	2. REPORT DATE	3. REPORT TYPE AND DATES COVERED
	February 15, 1993	Final 11 Jun 92 - 14 Dec 92

4. TITLE AND SUBTITLE

Kinetics of Nitric Oxide Formation Behind 3 to 4 km/s Shock Waves

5. FUNDING NUMBERS

DAAL03-92-K-0008

6. AUTHOR(S)

Charles E. Treanor and Marcia J. Williams

7. PERFORMING ORGANIZATION NAME(S) AND ADDRESS(ES)

Calspan-UB Research Center
4455 Genesee Street
P. O. Box 400
Buffalo, NY 14225

8. PERFORMING ORGANIZATION REPORT NUMBER

9. SPONSORING / MONITORING AGENCY NAME(S) AND ADDRESS(ES)

U. S. Army Research Office
P. O. Box 12211
Research Triangle Park, NC 27709-2211

10. SPONSORING / MONITORING AGENCY REPORT NUMBER

ARO 30404.1-EG-SDI

11. SUPPLEMENTARY NOTES

The view, opinions and/or findings contained in this report are those of the author(s) and should not be construed as an official Department of the Army position, policy, or decision, unless so designated by other documentation.

12a. DISTRIBUTION / AVAILABILITY STATEMENT

Approved for public release; distribution unlimited.

12b. DISTRIBUTION CODE

13. ABSTRACT (Maximum 200 words)

A previously published group of O_2/N_2 shock-tube experiments, wherein the time history of the NO 5 μm radiation was measured, has been studied to elicit information about the relevant chemical reactions which produce the radiation. It was found that the calculated radiation was sensitive to the rates used in the Zeldovich mechanism for NO formation, and that the rate measured by Monat et al. for $N_2 + O \longrightarrow NO + N$ produced important features of the observed radiation. Vibration-dissociation coupling in this reaction modifies the radiation history in an important way, and is an essential element in obtaining agreement with the experiment. To improve agreement over a range of O_2/N_2 mixtures, it was necessary to take into account the faster vibrational relaxation of N_2 by O_2 and O collisions and the subsequent effect on vibration-dissociation coupling.

14. SUBJECT TERMS

Reaction Rates
Air Chemistry
Nitric Oxide Formation
Vibration-Dissociation Coupling
Nitric Oxide Radiation

15. NUMBER OF PAGES

31

16. PRICE CODE

17. SECURITY CLASSIFICATION OF REPORT	18. SECURITY CLASSIFICATION OF THIS PAGE	19. SECURITY CLASSIFICATION OF ABSTRACT	20. LIMITATION OF ABSTRACT
UNCLASSIFIED	UNCLASSIFIED	UNCLASSIFIED	UL

NSN 7540-01-280-5500

Standard Form 298 (Rev 2-89)
Prescribed by ANSI Std Z39-18
298-102

TABLE OF CONTENTS

DTIC QUALITY INSPECTED 5

Accesion For		
NTIS CRA&I	☑	
DTIC TAB	☐	
Unannounced	☐	
Justification		
By _____		
Distribution /		
Availability Codes		
Dist	Avail and / or Special	
A-1		

i

LIST OF FIGURES

1. INTRODUCTION

The radiation behind a shock wave in a shock tube has frequently been used to simulate the radiation behind the bowshock of a missile. A simulation of this type was performed in a CUBRC program sponsored by the Army Research Office[1], where the missile velocity was in the range of 3-4 km/s at altitudes above 40 km. The purpose of that program was to determine the ultraviolet emission that could be expected from a planned flight experiment[2,3,4], and to gain a fundamental understanding of the physical processes that cause the radiation. The experiments were performed for a range of O_2/N_2 mixtures and shock velocities, and the ultraviolet and infrared radiation was measured. The purpose of the work reported here is to provide further analysis of the time history of the infrared radiation that was observed in these shock-tube experiments, and to elucidate the kinetic mechanisms behind the shock front.

In Ref. 5, Camac et al reported a set of shock-tube experiments in air in the same velocity and density range as those of Ref. 1. An earlier set of chemical rate constants suggested by Wray[8] was modified by Camac et al based on their time history of the infrared radiation. Using these rates, calculated infrared radiation profiles did not reproduce the experimental results of Ref. 1. In particular, the Camac rates did not produce the maxima of NO infrared radiation that were observed. In the present study a wide range of chemical rates was explored, and the effect of vibration-dissociation coupling in the chemical reactions was also investigated. Rates giving the best agreement with experiment are presented.

In Section 2 the infrared data of Ref. 1 are reviewed. In Section 3 the chemical variables that are available for adjustment are specified. In Section 4 the general relaxation process is described, and in Section 5 the effect of specific changes in the rate constants is demonstrated. Section 6 summarizes the analysis and presents the conclusions of the study.

2. EXPERIMENTAL DATA

The data that are examined in the present study were obtained in sixteen shock-tube experiments that used several different N_2/O_2 mixtures. Twelve of these experiments involved shock waves into gas mixtures at 2.25 torr pressure (40 km), and the mixture ratios, shock velocities and run numbers are listed in Table 1.

1

5%O_2/95%N_2		22.3%O_2/77.7%N_2		40%O_2/60%N_2	
Velocity km/sec	Run #	Velocity km/s	Run #	Velocity km/s	Run #
3.87	147	3.85	132	3.85	135
3.49	146	3.52	133	3.47	137
3.15	145	3.26	134	3.24	136
2.97	144	2.99	141	3.06	139

TABLE 1. Shock-wave experiments[1] into gas at p_0=2.25 torr.

The measured infrared radiation profiles for the experiments are given in Ref. 1, and are reproduced in Appendix A. A smooth line is drawn through each profile. These lines are used to represent the experiments in subsequent comparisons with calculated profiles.

Test conditions for the other four experiments are given in Table 2, with initial pressures of 4 torr (36 km), and 1 torr (46 km). Results for the experiments shown in Table 2 were not included in Ref. 1, but are shown in Appendix A.

Mixture	p_0 (torr)	Velocity	Run #
5%O_2/95%N_2	1.0	3.02 km/s	149
5%O_2/95%N_2	1.0	3.15 km/s	150
22.3%O_2/77.7%N_2	4.0	3.57 km/s	143
40%O_2/60%N_2	4.0	3.60 km/s	142

TABLE 2. Shock-wave experiments with p_0 = 1.0 and 4.0 torr.

As described in Ref. 1, the observed in-band infrared radiation is related to the NO concentration and the gas translational temperature through the relation

$$S=1.29 \times 10^{-20} \, L \, n_{NO} \, [1 - 3.21 \times 10^{-4} \, (T-3000)] \, \frac{watts}{cm^2 \, sr} \qquad (1)$$

with n_{NO} in molecules/cm^3, L in cm and T in degrees Kelvin. For these experiments, L, the shock-tube diameter, has the value of 7.62 cm. Throughout this report, the experimental radiation profiles

have been compared with profiles of S/L calculated from Eq. 1 and values of n_{NO} and T determined by the Marrone-Garr[6] normal shock program.

3.   CHEMICAL EQUATIONS

The gas behind the shock wave is heated to high temperatures (4000-8000K), and the O_2 and N_2 react chemically to form oxygen and nitrogen atoms, nitric oxide, nitric oxide ions, and electrons. The rate at which the chemical reactions occur was calculated with the Marrone-Garr normal-shock program[6]. The reactions considered are shown in Table 3:

1. $O_2 + O.$	$\rightleftharpoons$	$2O + O$
2. $O_2 + O_2$	$\rightleftharpoons$	$2O + O_2$
3. $O_2 + M$	$\rightleftharpoons$	$2O + M$
4. $N_2 + N$	$\rightleftharpoons$	$2N + N$
5. $N_2 + N2$	$\rightleftharpoons$	$2N + N_2$
6. $N_2 + M$	$\rightleftharpoons$	$2N + M$
7. $NO + M$	$\rightleftharpoons$	$N + O + M$
8. $N + O_2$	$\rightleftharpoons$	$NO + O$
9. $O + N_2$	$\rightleftharpoons$	$NO + N$
10. $NO^+ + e$	$\rightleftharpoons$	$N + O$

TABLE 3. Chemical Reactions

The reaction rate for each reaction is represented in the form

$$k_j = A_i T^{B_i} e^{-C_i/T} \tag{2}$$

and M is taken to represent all species not specified in parallel reactions. In the temperature and pressure range of these experiments, the chemistry is dominated by Reactions 1, 2, 3, 8 and 9.

The normal-shock program[6] uses a single rotational-translational temperature, but allows for vibrational relaxation of the molecular species. Each species relaxes with a single vibrational relaxation time, and sustains a distinctive vibrational temperature during relaxation, relaxing according to the relation

3

$$\frac{d\varepsilon\ (T_{v_i})}{dt} = \frac{\varepsilon\ (T) - \varepsilon\ (T_{v_i})}{\tau_i\ (T)} \tag{3}$$

$\varepsilon(T_{v_i})$ is the vibrational energy of species i at vibrational temperature T_{v_i}, and $\varepsilon(T)$ is the vibrational energy it would have at the translational-rotational temperature T. τ_i is the single vibrational relaxation time for the ith species. The product of the relaxation time and the pressure in the shock tube is taken in the form

$$\tau_{ik}\ p = a_{ik}\ T^{b_{ik}}\ e^{c_{ik}/T^{1/3}}\quad \text{(atm-s)} \tag{4}$$

where the constants a, b and c depend on the relaxing molecule (i) and the colliding molecule (k). A compilation of experimental values of coefficients is given in Ref. 7.

4. RELAXATION PROCESS BEHIND SHOCK WAVES

A shock wave into an O_2/N_2 mixture, in the 3-4 km/s velocity range, is known to produce the following chemical sequence. The temperature is very high immediately behind the shock, and O_2 and N_2 begin vibrational relaxation. The O_2 begins to dissociate (Reactions 1-3), and this dissociation can be delayed for a time of the order of the O_2 vibrational relaxation time by the effect of vibration-dissociation coupling. The oxygen atoms produced from this dissociation react with N_2 in an endothermic reaction to form nitric oxide and nitrogen atoms (Reaction 9). As pointed out in the analysis which follows, this reaction can be delayed for a time of the order of the N_2 vibrational relaxation time by vibration- dissociation coupling. As nitrogen atoms are formed, they react quickly in an exothermic reaction with O_2 (Reaction 8) to form NO and oxygen atoms. This sequence of Reactions 9 and 8 can be described by

Reaction 9 $\qquad O + N_2 \rightleftharpoons NO + N$

$$Q_9 = \left(\frac{dn_{NO}}{dt}\right)_9 = \left(\frac{dn_N}{dt}\right)_9 = k_{f9}\ n_O\ n_{N_2}\left[1 - \frac{1}{K_9}\left(\frac{n_{NO}n_N}{n_O n_{N_2}}\right)\right] \tag{5}$$

Reaction 8 $\qquad N + O_2 \rightleftharpoons NO + O$

$$Q_8 = \left(\frac{dn_{NO}}{dt}\right)_8 = -\left(\frac{dn_N}{dt}\right)_8 = k_{f8}\ n_N\ n_{O_2}\left[1 - \frac{1}{K_8}\left(\frac{n_{NO}n_O}{n_N n_{O_2}}\right)\right] \tag{6}$$

4

where K_8 and K_9 are the equilibrium constants for Reactions 8 and 9.

Since Reaction 9 is the only appreciable source of nitrogen atoms (Reactions 4 through 7 are relatively slow at these temperatures), a quasi-steady state is soon established by Reactions 8 and 9, in which $Q_8 = Q_9$. Setting these terms equal, using this relation to eliminate n_N in one of the equations and using the relation

$$\frac{dn_{NO}}{dt} = \left(\frac{dn_{NO}}{dt}\right)_8 + \left(\frac{dn_{NO}}{dt}\right)_9 \qquad (7)$$

gives

$$\frac{dn_{NO}}{dt} = 2\, n_O \left[\left(n_{O_2}\, n_{N_2} - \frac{(n_{NO})^2}{K_8\, K_9} \right) \bigg/ \left(\frac{n_{O_2}}{k_{f_9}} + \frac{n_{NO}}{k_{f_8}\, K_9} \right) \right] \qquad (8)$$

In the early part of the reaction the value of n_{NO} is small, and the second term in the numerator is negligible. The derivative dn_{NO}/dt increases as n_O increases. As n_{NO} becomes appreciable, the numerator factor $[n_{O_2}n_{N_2} - (n_{NO})^2/(K_8K_9)]$ begins to decrease, so that dn_{NO}/dt reaches a maximum and then decreases. When the numerator reaches zero, dn_{NO}/dt is zero, and n_{NO} is at its maximum value. Following this the numerator is negative, and n_{NO} decreases. Finally, the numerator again becomes equal to zero when n_{NO} reaches its equilibrium value.

In all of the experiments this sequence of growth of NO radiation to a maximum and subsequent relaxation to equilibrium is clearly shown in the radiation records. The mild temperature effect (Eq. 1) does not change these general features. The salient reference points in this process are shown in Figure 1.

5.   RATE CONSTANT VARIATIONS

There is general agreement among previous research results regarding the values of the constants B_i and C_i to be used in Eq. 2. In the present work, the values of A_i were systematically varied to ascertain the effect on the NO infrared radiation. However, variation of these constants did not lead to a single set of values which produced results consistent with all of the experiments. The effect of vibration-dissociation coupling was then considered, and this provided a striking improvement when coupling of N_2 vibration in Reaction 9 ($N_2 + O \rightleftarrows NO + N$) was included.

It was still not possible, however, to fit data for the different O_2/N_2 mixtures with a single set of rate constants. Since the effects of O_2 and O as collision partners in providing N_2 vibrational relaxation are known to be faster than that of N_2, variations in these values were considered. It was found that if O_2 and O are taken to be more effective than N_2 in the vibrational relaxation of N_2, greatly improved agreement can be obtained. The separate steps in the data analysis are described below.

As discussed in Ref. 1, Camac et al[5] reports a series of infrared experiments in the same velocity/density range as those in Ref. 1. They concluded that the best values for the reaction rate constants were those given in Table 4.

Reaction	A	B	C
1	1.5×10^{-4}	-1.0	59380
2	5.4×10^{-5}	-1.0	59380
3	1.2×10^{-5}	-1.0	59380
4	6.8×10^{-2}	-1.5	113200
5	8.0×10^{-7}	-0.5	113200
6	3.2×10^{-7}	-0.5	113200
7	6.6×10^{-4} *	-1.5	75490
8	2.2×10^{-14}	1.0	3565
9	5.0×10^{-11}	0	38016
10	9.0×10^{-3}	-1.5	0

TABLE 4. Reaction-Rate Constants, Camac et al[5] $k_{f_1} \, AT^B e^{-C/T}$ (cm^3/molec-s)

* This number was reported incorrectly in Ref. 1.

These rates, however, when used to calculate the NO infrared radiation, gave results much different from the Ref. 1 data. As shown in Figure 2, the rates of Table 4 do not produce the maxima that are shown in many of the experimental profiles, and give a poor representation of the rate of growth.

The rates recommended by Camac et al[5] were a modification of those suggested by Wray[8]. The modifications consisted of elimination of the reaction

$$N_2 + O_2 \xleftrightarrow{\quad} 2NO \qquad (9)$$

6

based on a separate set of experiments, and a decrease in Wray's value of A_9 by a factor of 2.3. The decrease in A_9 was suggested in order to explain the long incubation times observed in the experiments of Ref. 5. The effect on the longer-time history of the radiation was not considered, because at longer times the radiation was thought to be affected by boundary-layer growth in the small (1.5 inch) diameter shock tube.

In fact, Wray's value of A_9 (and elimination of the reaction shown in Eq. 9) gives a much better fit to the data of Ref. 1, as shown in Figure 3. The larger value of A_9 results in NO radiation maxima that are not present with calculations using the Ref. 1 value. However, the details do not agree with the experiments, especially at the lower speeds.

More-recent experiments to measure the value of A_9 have been reported by Monat et al[9]. These experiments gave a value

$$A_9 = 3.0 \times 10^{-10} \ cm^3 / \ molec\text{-}s \qquad (10)$$

This value provides a better fit to the experiments, especially at the lower speeds, as shown in Figure 4. However, at the higher speeds, particularly at the lower oxygen concentrations, it produces a much-too-rapid rise in NO, and too large a maximum. The Monat value of A_9 was retained in subsequent calculations.

A recent experiment was performed by Jerig et al[10] to measure the dissociation rate of O_2 in collisions with N_2. They report a value for $A_{O_2\text{-}N_2}$ of

$$A_{O_2\text{-}N_2} = 5.6 \times 10^{-6} \ (\pm 25 \ \%) \ cm^3\text{-}{}^\circ K / \ molec\text{-}s \qquad (11)$$

which is about half the Camac value. Use of this value in Reaction 3 decreases the rate of production of oxygen atoms at very early times, but Reaction 8 soon becomes the dominant O-atom producer, and there is little net effect on the NO production. Results are shown in Figure 5. Therefore at this point the higher Camac value of A_3 was restored to the rate model for further attempts to fit the experimental data.

The next variation that was considered was the effect of vibration - dissociation coupling. The simplest model that encompasses this effect is that suggested by Park[11], where the operative temperature in the dissociation process is taken to be $T^x T_v^{1-x}$. The value of x was chosen[12] as 0.5

or 0.7, based on examination of experiments with strong shockwaves. In the calculations reported here a value of x=0.7 was used.

Vibrational relaxation of the O_2 and N_2 molecules was accounted for in the program through the use of Eqs.3 and 4. The constants used to determine τp for N_2 and O_2 are given in Table 5.

	a	b	c	Ref.
N2	1.1×10^{-11}	0.5	154	(13,6)
O2	1.6×10^{-9}	0	101.4	(13,6)

TABLE 5. Vibrational Relaxation Parameters for Equation 4.

The vibrational relaxation of NO is known to be very fast[5,14,15], so that NO was taken to be in local vibrational equilibrium.

Coupling of vibration and dissociation in the oxygen dissociation reactions (Reactions 1 - 3) has only a minor effect on the outcome, since the vibrational relaxation of O_2 is completed before appreciable NO is formed. However, coupling has a strong effect on Reaction 9, where the formation of NO from N_2 and O can be delayed by the slow vibrational relaxation of N_2. Camac et al[5] had considered this effect, but concluded that they could not obtain information on coupling from their data. However, using Park's[11] coupling formula for Reaction 9, with a value of x = 0.7, the NO rise in the higher-speed shocks is slowed considerably (see Figure 6), giving much better agreement in the high-speed experiments and having relatively little effect on the slower shocks. It can be seen that the coupling is most important in Reaction 9; when the coupling is introduced into all the endothermic reactions, there is relatively little further change, as shown in Figure 7. It was concluded that this vibration-dissociation coupling is a necessary ingredient in the explanation of the observed NO radiation, and it was included in Reactions 1 through 6 and 9 in subsequent calculations. It should be pointed out that Monat's experiments were performed under conditions where this coupling term is not involved, so that a separate check on this feature cannot be obtained.

Figure 6 demonstrates a marked variation in agreement for different N_2/O_2 mixtures, particularly for the high-speed shocks. Because of the sensitivity of the calculated radiation to vibration-dissociation coupling in Reaction 9, this variation could be related to the more effective vibrational relaxation of N_2 by O_2 and O as compared with N_2. The effectiveness of oxygen

8

molecules in causing vibrational relaxation of nitrogen has been measured[16] to be some 2.5 times greater than that of nitrogen molecules, and oxygen atoms have been reported[17] to be much more effective than N_2 at lower temperatures.

The computer program used in the current work[6] was not capable of accounting for more than one relaxation time for each molecule, so that a direct check of this variable was not possible. It was possible, however, to adjust the single relaxation time to account approximately for the O_2 and O content, by using an averaged relaxation time for N_2 vibrational relaxation. Thus if τ_{N_2} is taken as

$$\frac{1}{\tau_{N_2}} = \left(\frac{n_{O_2}}{n_{O_2} + n_{N_2}}\right)\frac{1}{\tau_{N_2 O_2}} + \left(\frac{n_{N_2}}{n_{O_2} + n_{N_2}}\right)\frac{1}{\tau_{N_2 N_2}} \tag{12}$$

an approximate relaxation time for the various O_2/N_2 mixtures can be obtained, by testing various values of P, where

$$P = \frac{\tau_{N_2 O_2}}{\tau_{N_2 N_2}} \tag{13}$$

The value used for $\tau_{N_2 N_2}$ was the one previously used for τ_{N_2} as given in Table 5. Figure 8 demonstrates the improved calculation for P = 0.3, and Figure 9 shows further improvement for P = 0.2. All of the calculated NO radiation peaks have essentially the correct maximum value, and reach this value at close to the correct time. For the fastest shocks the calculated times to the maximum are two to three microseconds shorter than the experimental values. It is not expected that this can be attributed to the time response of the experiment, which is the order of one microsecond.

At this point the slower value of $A_{O_2-N_2}$ measured by Jerig et al[10] was again used in the calculation of k_{f3}. The results are shown in Figure 10. It can be seen that this did not improve the agreement, so the Camac value was restored to the rate model.

After these adjustments in the parameters were applied to the infrared profile calculations for the twelve p_0=2.25 torr experiments, the same model was used to calculate profiles for the four experiments described in Table 2. The Monat[9] rate was used, along with the coupling factor x = 0.7 and the nitrogen vibration factor P = 0.2. The results are shown in Figure 11. For the 4-torr experiments the calculated radiation profile rises slightly more rapidly than the experimental value, as is the case for the 2.25-torr experiments, but produces essentially the correct profile and

9

maximum intensity. The two 1-torr experiments may show some effect of boundary layer growth in the shock tube, which tends to distort the time scale of the recorded profile[5]. However, the general pattern and scale of the radiation is reproduced well, and the sensitivity of the radiation to a small change in velocity is reflected in the calculation.

6.   SUMMARY AND CONCLUSIONS

A group of O_2/N_2 shock-tube experiments[1], wherein the time history of the NO 5-um radiation was measured, have been studied to elicit information about the relevant chemical reactions which produce the radiation. The experiments covered a range of O_2/N_2 mixtures, and a velocity range from 3 to 4 km/sec; the initial pressure in the shock tube was 2.25 torr, with a few experiments at 1.0 and 4.0 torr, covering an altitude range of 36 to 46 km.

It was found that the calculated radiation was sensitive to the rates used in the Zeldovich mechanism for NO formation, and that the rate measured by Monat et al[9] for the reaction of N_2 and O in forming NO and N permits calculation of important features of the observed radiation. Vibrational relaxation of N_2, and the coupling of this relaxation with the N_2+O reaction, modifies the reaction rate in an important way for experiments in this velocity and density range. The translational temperature T was replaced by $T^{0.7}T_{vN_2}^{0.3}$ in the reaction rate equation. It was concluded that this coupling effect must be included in shocked-air calculations.

After these corrections, the NO intensity profiles still showed an unexplained dependence on the O_2/N_2 mixture ratio. It was found that consideration of the dependence of the N_2 vibrational relaxation rate on the relative amounts of O_2 and N_2 that are present, and the subsequent vibration-dissociation coupling, improves agreement between calculation and experiment.

The recent experimental results of Jerig et al[10] on the dissociation rate of O_2 by collision with N_2 cannot provide a clear comment on the correct value of k_{f3}.

ACKNOWLEDGEMENT

REFERENCES

1. Wurster, W. H., Treanor, C.E., Williams, M.J., Non-equilibrium Radiation from Shock-Heated Air, Final Report. U.S. Army Research Office, Contract No. DAAL03-88K-0174, July 1991, Calspan UB Research Center, Buffalo, NY.

2. Levin, D.A., Collins, R.J., Candler, G.V., Computations for Support Design of Measurements of Radiation from Low Velocity Shocked Air, J. Thermophysics and Heat Transfer $\underline{5}$ 463 (1991).

3. Levin, D.A., Candler, G.V., Collins, R.J., Erdman, P.W., Zipf, E., Espy, P, Howlett, C., Comparison of Theory with Experiment for the Bow Shock Ultraviolet Rocket Flight, J. Thermophysics and Heat Transfer $\underline{7}$ 30 (1993).

4. Erdman, P.W. Zipf, E.C., Espy, P. Howlett, C. Levin, D.A., Loda, R. Collins, R.J., Candler, G.V., Flight Measurements of Low-Velocity Bow Shock Ultraviolet Radiation, J. Thermophysics and Heat Transfer $\underline{7}$ 37 (1993).

5. Camac, M. Feinberg, R., and Teare, J.D., The Production of Nitric Oxide in Shock-Heated Air, Avco Research Report 245, Dec. 1966.

6. Marrone, P.V., Inviscid, Nonequilibrium Flow behind Bow and Normal Shock Waves, Part 1, General Analysis, CAL Report No. QM 1626-A-12(I) May 1963.

7. Millikan, R.C. and White, D.R., Systematics of Vibrational Relaxation, J. Chem. Phys., $\underline{39}$ 3209 (1963)

8. Wray, K. L., Progress in Astronautics and Rocketry, Edited by F.R. Riddell (Academic Press, New York 1962) Vol. 7, p. 181.

9. Monat, J.P., Hanson, R.K., and Kruger, C.H., Shock Tube Determination of the Rate Coefficient for the Reaction $N_2 + O \rightarrow NO + N$, Proceedings of the 17th Symposium (International) on Combustion, 1978, p. 543.

10. Jerig, L., Theilen, K., Roth, P., High-Temperature Dissociation of Oxygen Diluted in Argon or Nitrogen, AIAA Journal $\underline{29}$ 1136 (1991)

11. Park, C., Two-Temperature Interpretation of Dissociation Rate Data for O_2 and N_2, AIAA Paper 88-0458, 1988.

12. Nonequilibrium Hypersonic Aerodynamics, by Chul Park, John Wiley & Sons, 1990.

REFERENCES (cont.)

13. Blackman, V.H., Vibrational Relaxation in Oxygen and Nitrogen, J. Fluid Mech. 1 61 (1956).

14. Kamimoto, G. and Matsui, H., Vibrational Relaxation of Nitric Oxide in Argon, J. Chem. Phys. 53 3987 (1970)

15. Wray, K.L., Shock-Tube Study of the Vibrational Relaxation of NO, J. Chem. Phys. 36 2597 (1962)

16. Breshears, W.D. and Bird, P.F., Effect of Oxygen Atoms on the Vibrational Relaxation of Nitrogen, J. Chem. Phys. 48 4768 (1968)

17. Eckstrom, D.J., Vibrational Relaxation of Shock-Heated N_2 by Atomic Oxygen using IR Tracer Method, J. Chem. Phys. 59 2787 (1973).
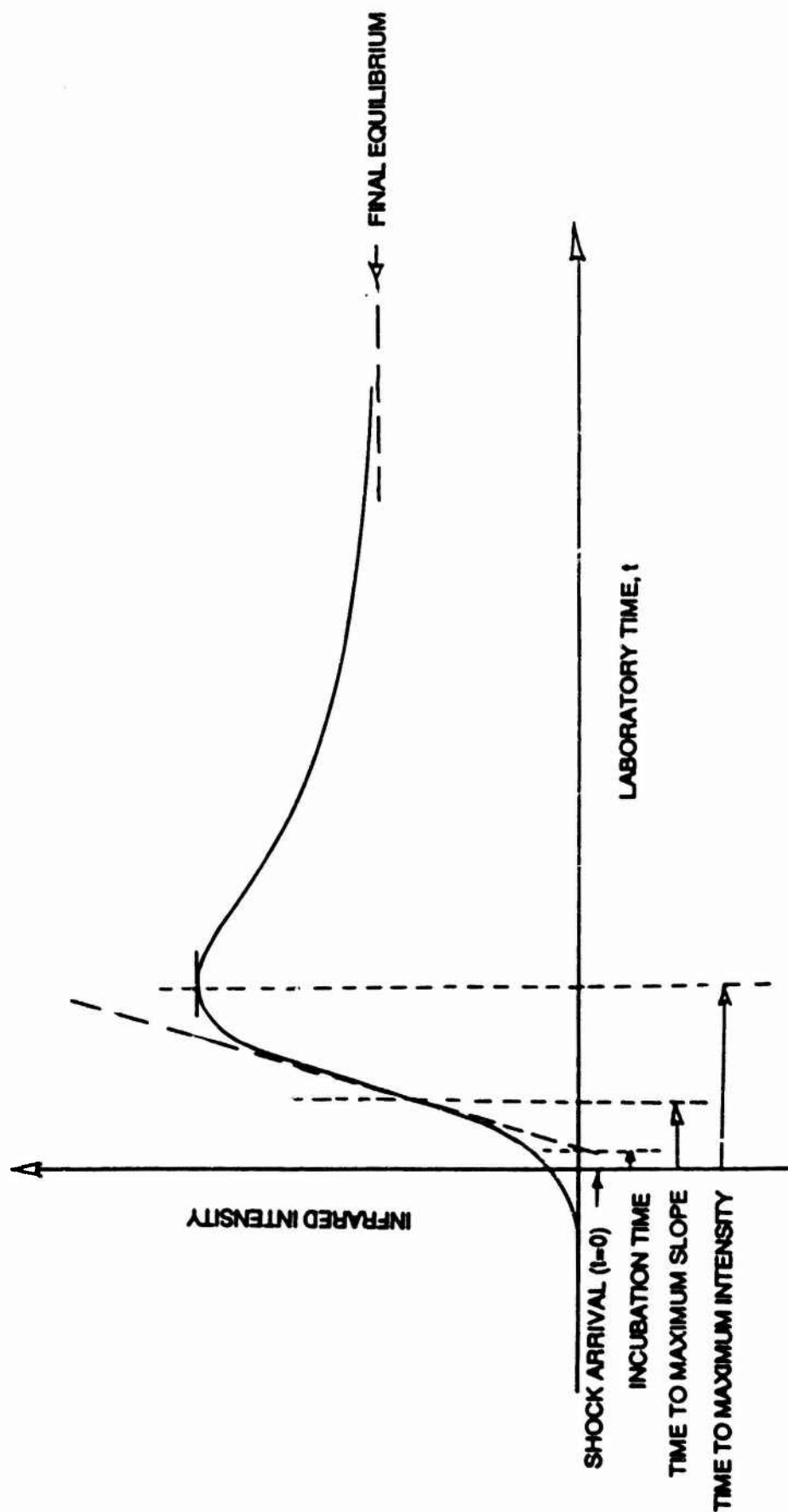
FIGURE 1. CHARACTERISTIC HISTORY OF NON-EQUILIBRIUM INFRARED RADIATION INTENSITY

13

$P_0 = 2.25$ torr

LAB TIME SCALE: 0 to 220 µs

5% O_2 / 95% N_2
INTENSITY SCALE: 0 to 6.0(-4) w/cm³-sr

$V_s = 3.87$ mm µs

147

22.3% O_2 / 77.7 % N_2
INTENSITY SCALE: 0 to 1.3(-3) w/cm³-sr

$V_s = 3.85$ mm/µs

132

40% O_2 / 60% N_2
INTENSITY SCALE: 0 to 1.5(-3) w/cm³-sr

$V_s = 3.85$ mm/µs

135

$V_s = 3.49$ mm/µs

146

$V_s = 3.52$ mm/µs

133

$V_s = 3.47$ mm/µs

137

14
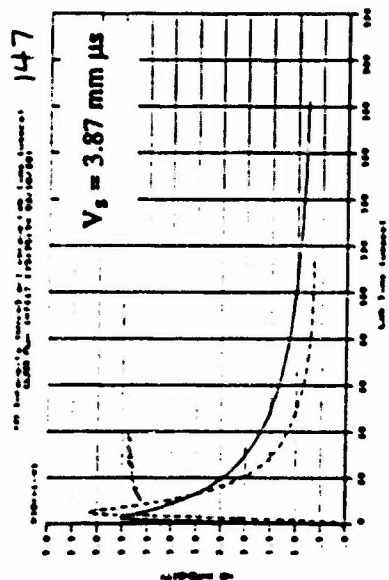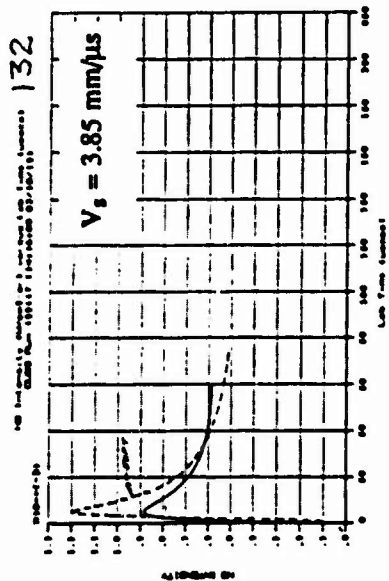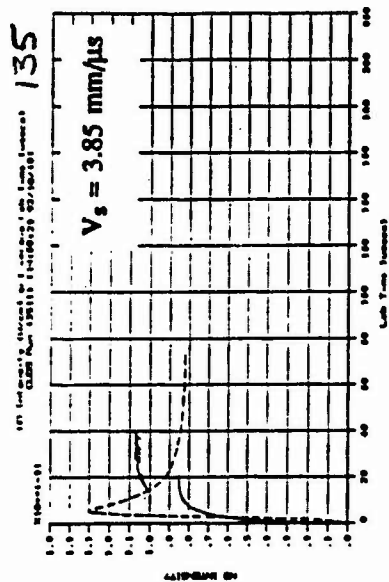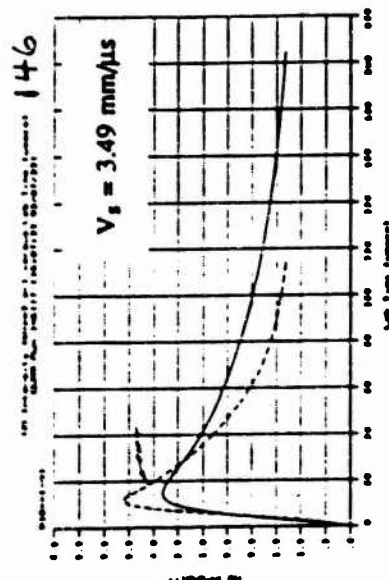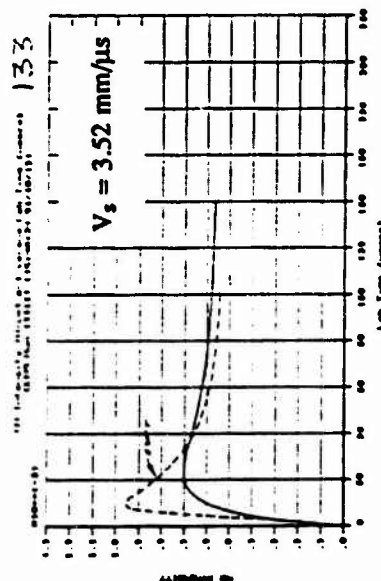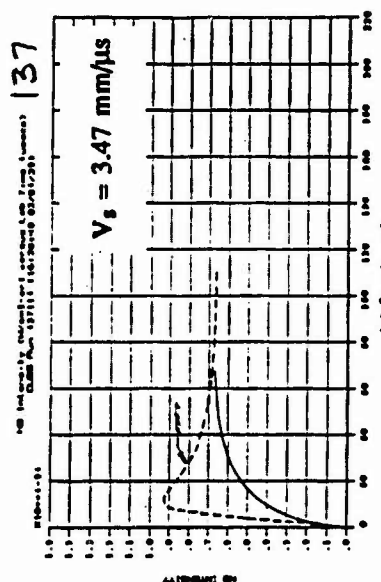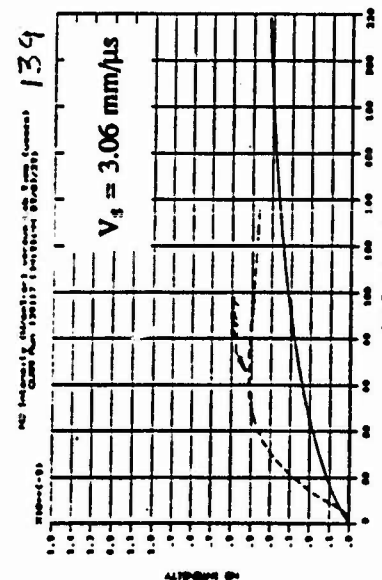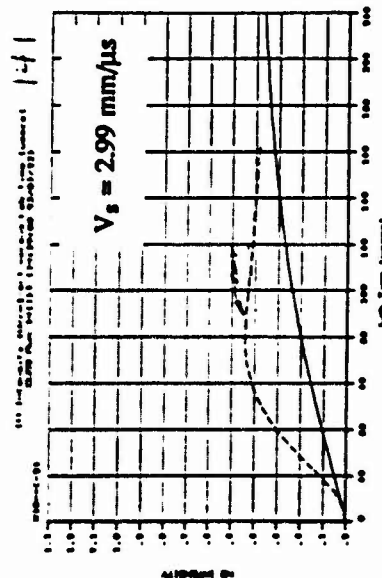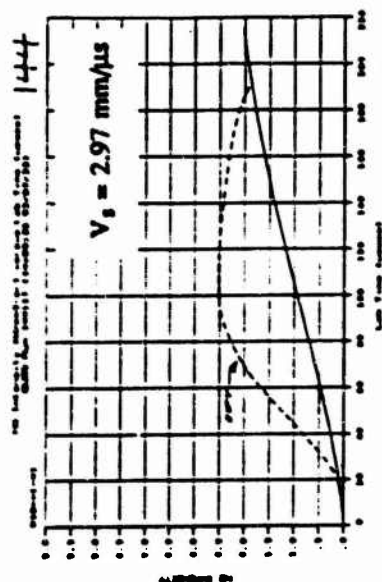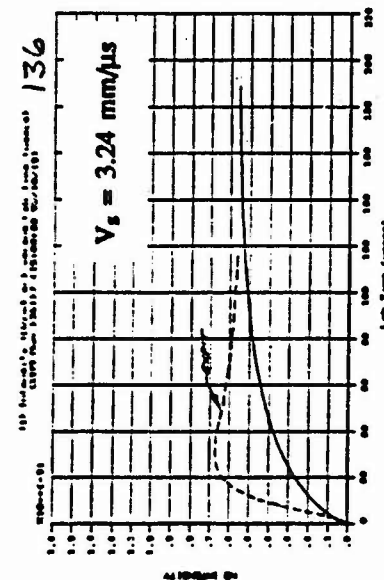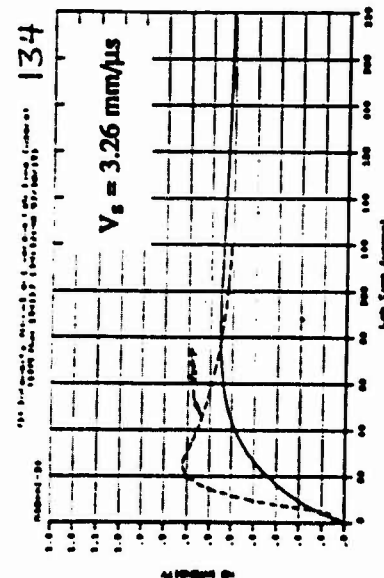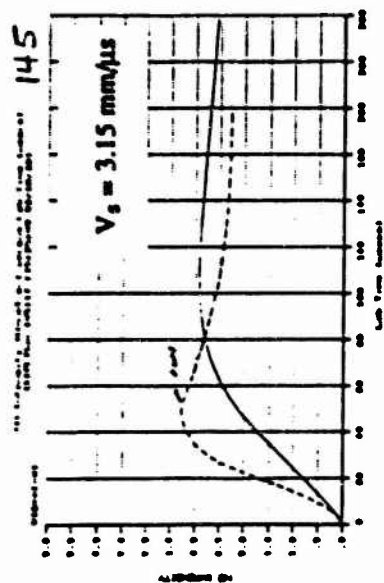
FIGURE 2. MEASURED AND CALCULATED 5.3 µm INTENSITY PROFILES

RATES FOR REACTIONS: 1-10   CAMAC (REF. 5)

(RUN NUMBER IN UPPER RIGHT CORNER OF EACH PLOT PROVIDES REFERENCE TO FULL-SCALE PROFILE IN APPENDIX A.)

15

$P_0 = 2.25$ torr

LAB TIME SCALE: 0 to 220 µs

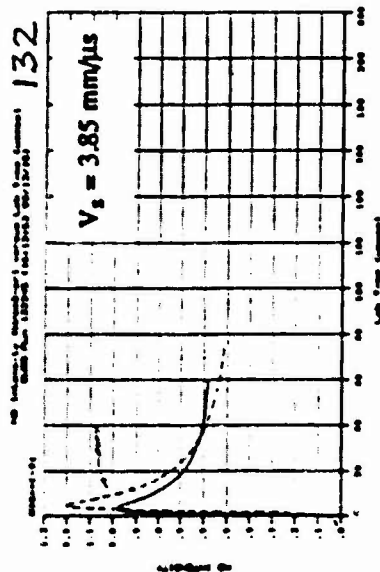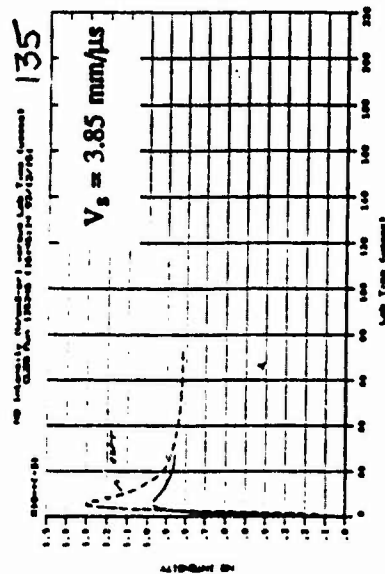**5% O$_2$ / 95% N$_2$**
INTENSITY SCALE: 0 to 6.0 (-4) w/cm^3-sr

22.3% O$_2$ / 77.7 % N$_2$
INTENSITY SCALE: 0 to 13(-3) w/cm^3-sr

40% O$_2$ / 60% N$_2$
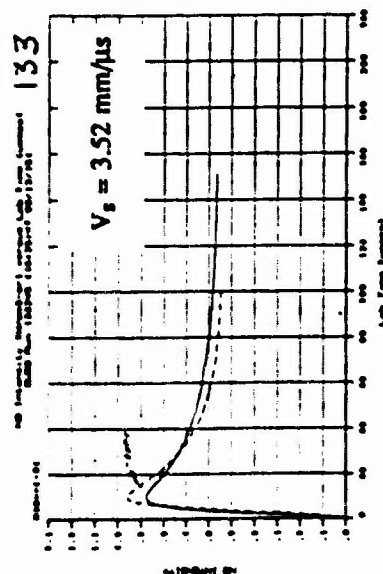INTENSITY SCALE: 0 to 1.5(-3) w/cm^3-sr

147 $V_s = 3.87$ mm/µs

132 $V_s = 3.85$ mm/µs

135 $V_s = 3.85$ mm/µs

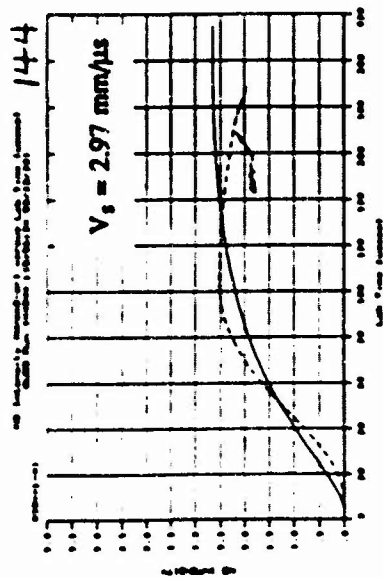146 $V_s = 3.49$ mm/µs

133 $V_s = 3.52$ mm/µs
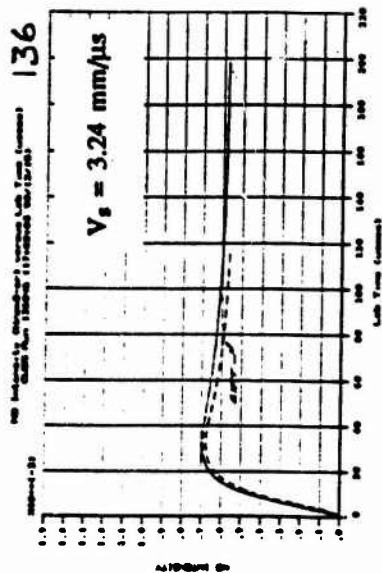
137 $V_s = 3.47$ mm/µs

16
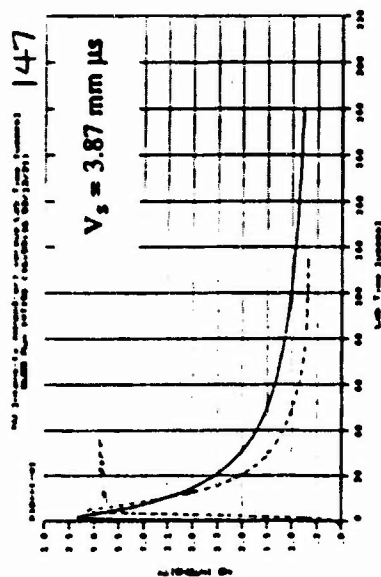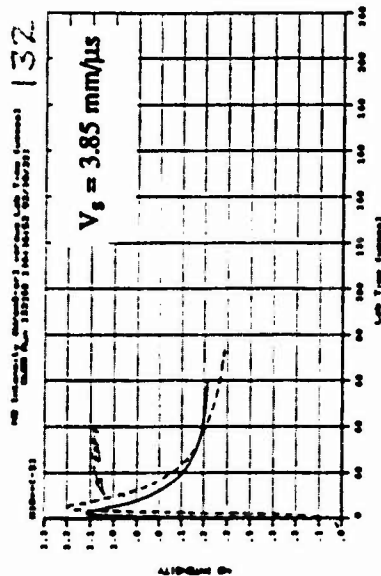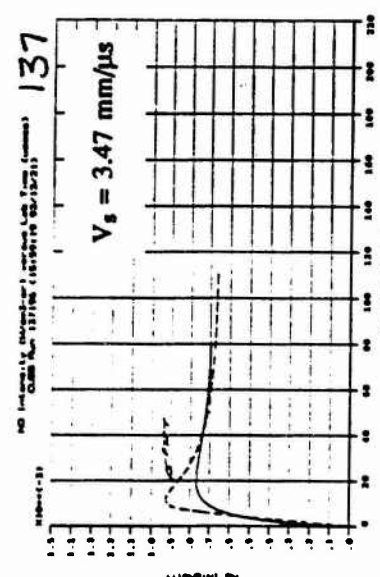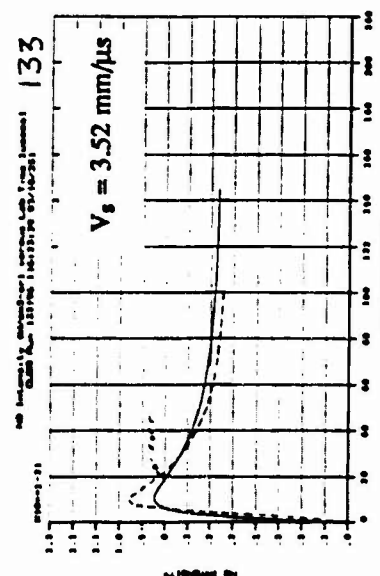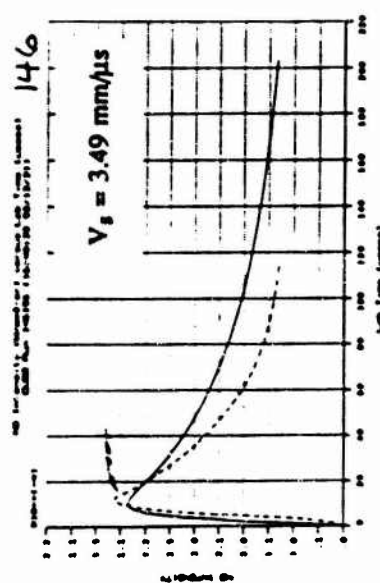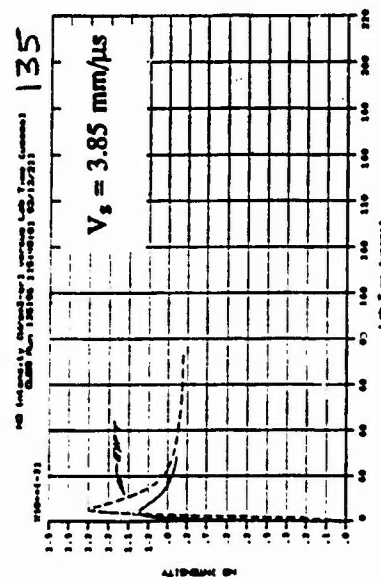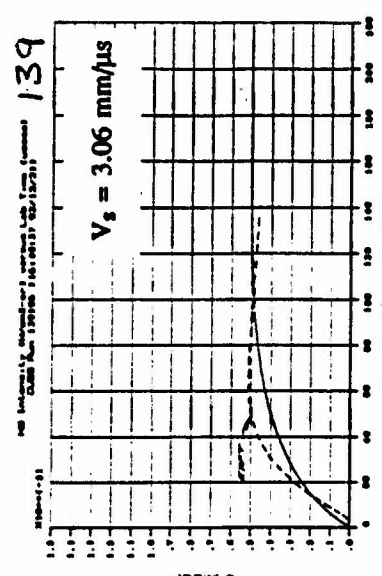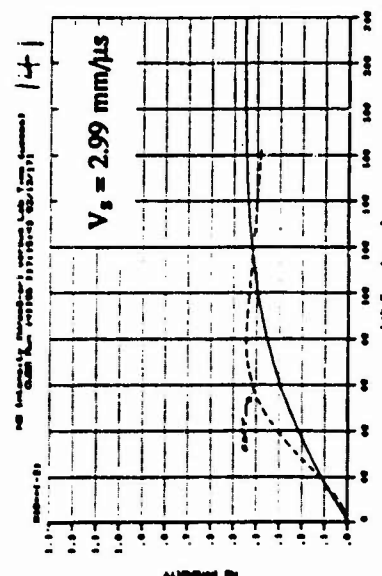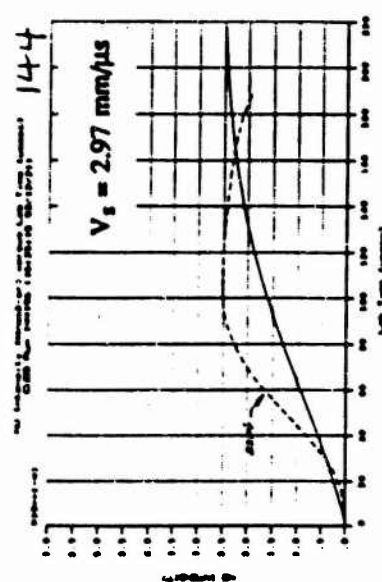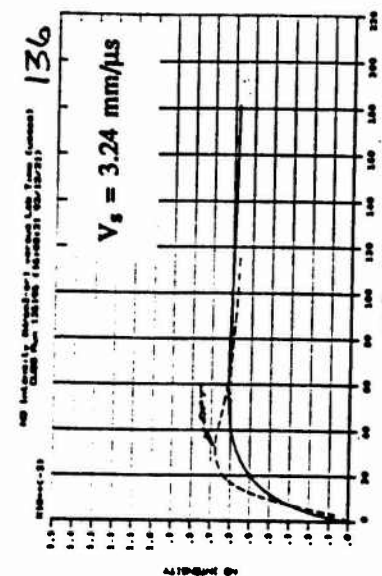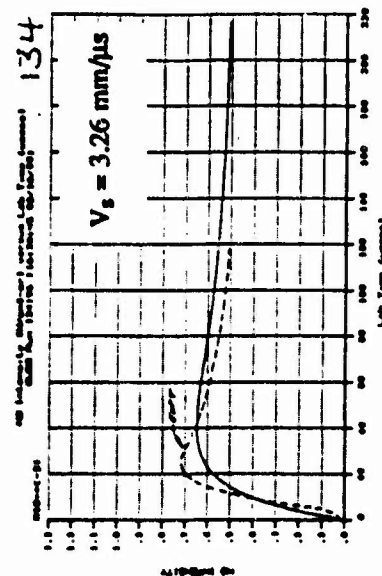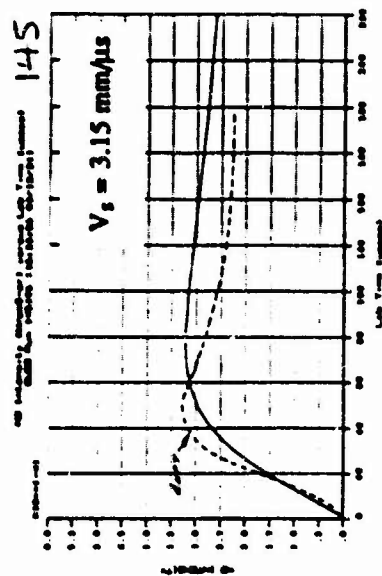
FIGURE 3. MEASURED AND CALCULATED 5.3 μm INTENSITY PROFILES

RATES FOR REACTIONS: 1-8,10   CAMAC (REF. 5)
                        9   WRAY (REF. 8), i.e. 2.3 TIMES CAMAC'S RATE

(RUN NUMBER IN UPPER RIGHT CORNER OF EACH PLOT PROVIDES REFERENCE TO FULL-SCALE PROFILE IN APPENDIX A.)

17

$P_o = 2.25$ torr

LAB TIME SCALE: 0 to 220 μs

22.3% O_2 / 77.7 % N_2
INTENSITY SCALE: 0 to 1.3(-3) w/cm^3-sr

40% O_2 / 60% N_2
INTENSITY SCALE: 0 to 1.5(-3) w/cm^3-sr

5% O_2 / 95% N_2
INTENSITY SCALE: 0 to 6.0 (-4) w/cm^3-sr

135 — $V_s = 3.85$ mm/μs

132 — $V_s = 3.85$ mm/μs

137 — $V_s = 3.47$ mm/μs

133 — $V_s = 3.52$ mm/μs

147 — $V_s = 3.87$ mm/μs

146 — $V_s = 3.49$ mm/μs

18
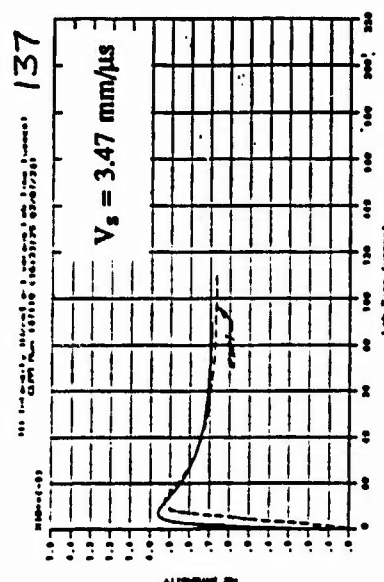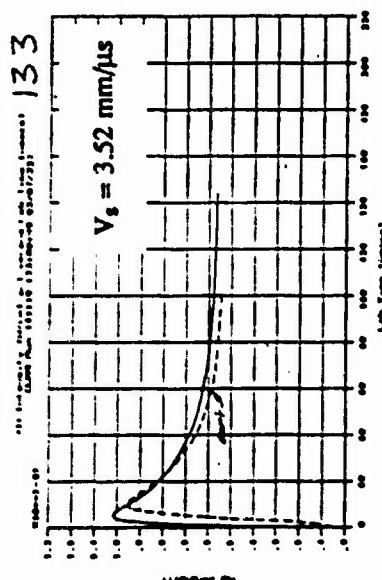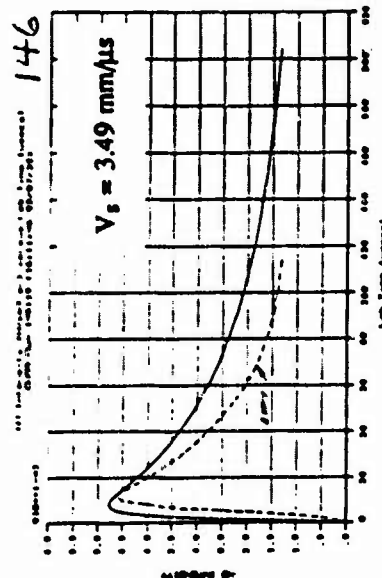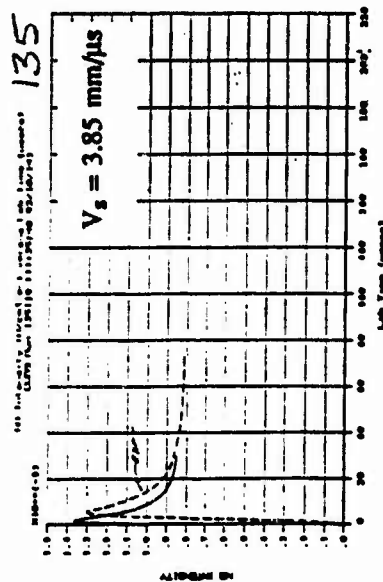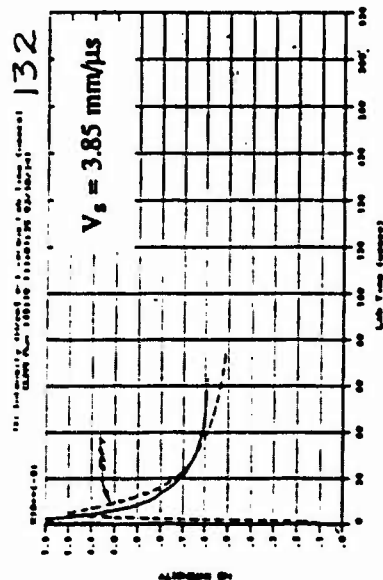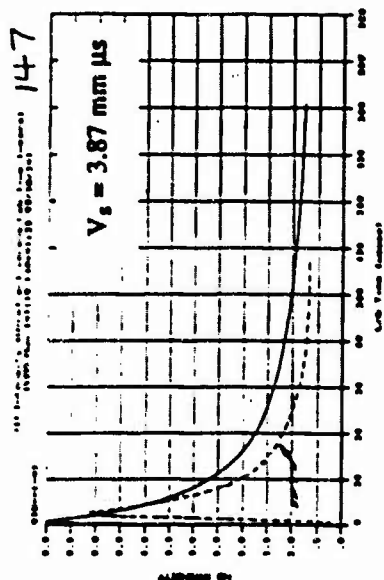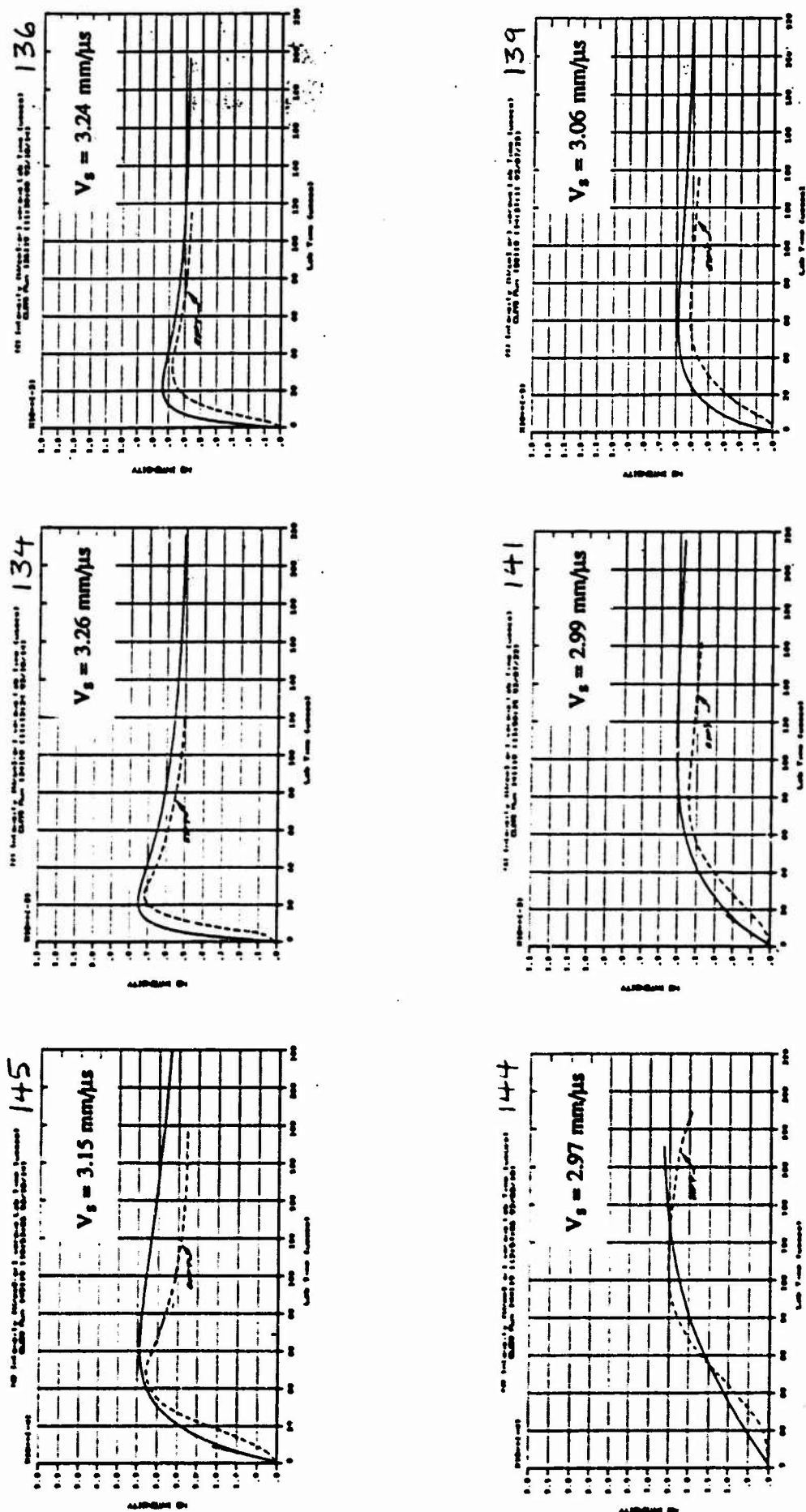
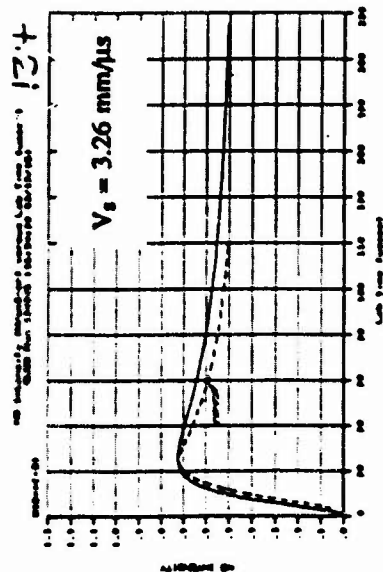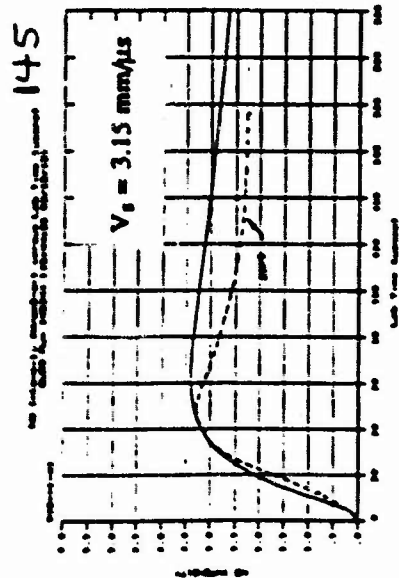FIGURE 4. MEASURED AND CALCULATED 5.3 μm INTENSITY PROFILES

RATES FOR REACTIONS: 1-8,10   CAMAC (REF. 5)
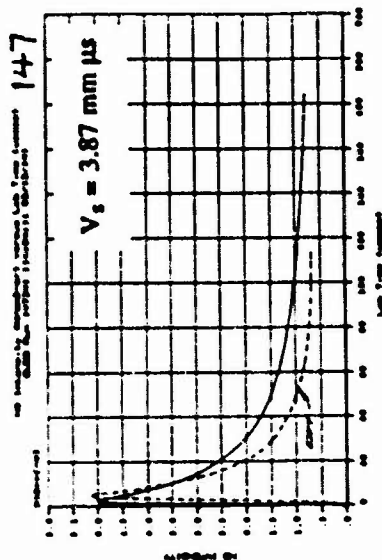   9   MONAT (REF. 9), i.e. 2.71 TIMES CAMAC'S RATE

(RUN NUMBER IN UPPER RIGHT CORNER OF EACH PLOT PROVIDES REFERENCE TO FULL-SCALE PROFILE IN APPENDIX A.)
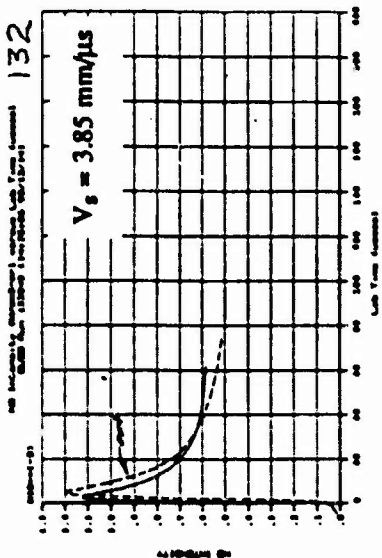
19

P₀ = 2.25 torr

LAB TIME SCALE: 0 to 220 μs

22.3% O₂ / 77.7 % N₂
INTENSITY SCALE: 0 to 1.3(-3) w/cm³-sr

40% O₂ / 60% N₂
INTENSITY SCALE: 0 to 1.5(-3) w/cm³-sr

5% O₂ / 95% N₂
INTENSITY SCALE: 0 to 6.0 (-4) w/cm³-sr

V_s = 3.87 mm μs   147

V_s = 3.85 mm/μs   132

V_s = 3.85 mm/μs   135

V_s = 3.49 mm/μs   146

V_s = 3.52 mm/μs   133

V_s = 3.47 mm/μs   137

20
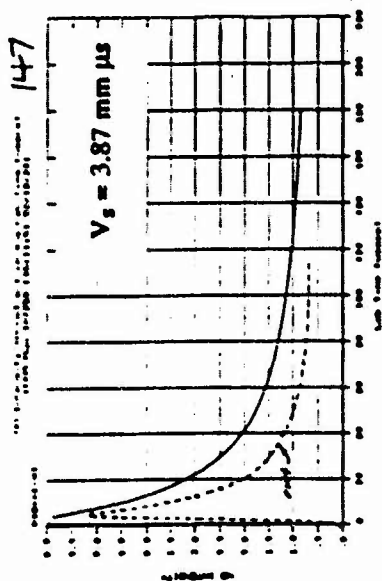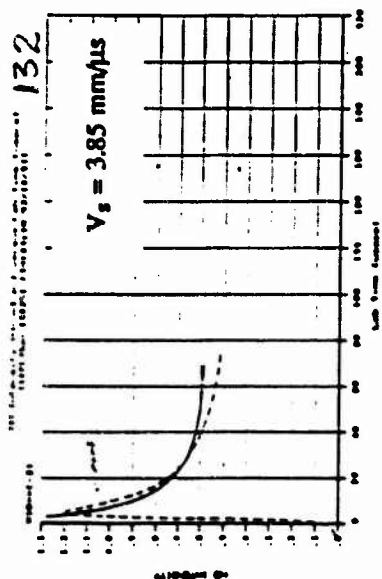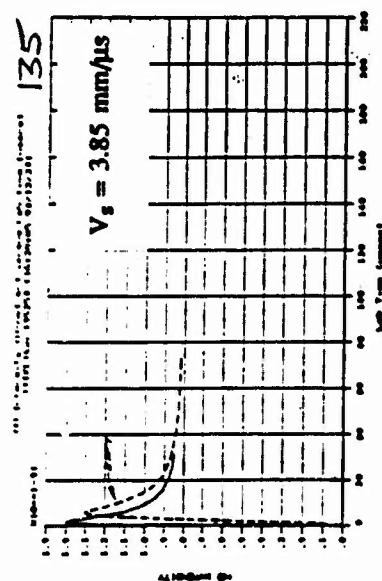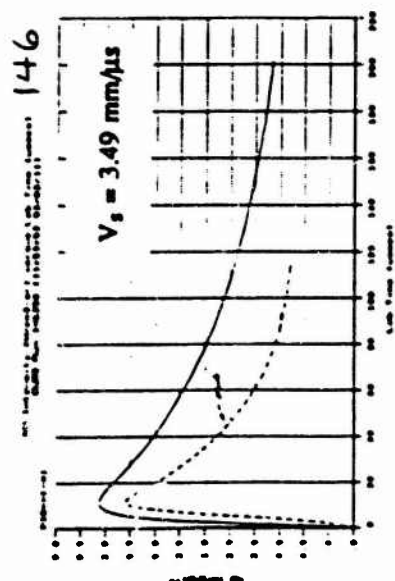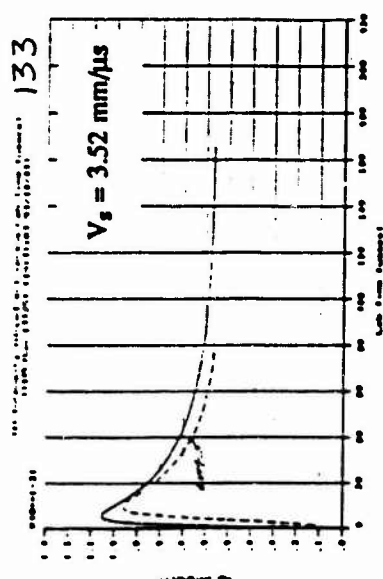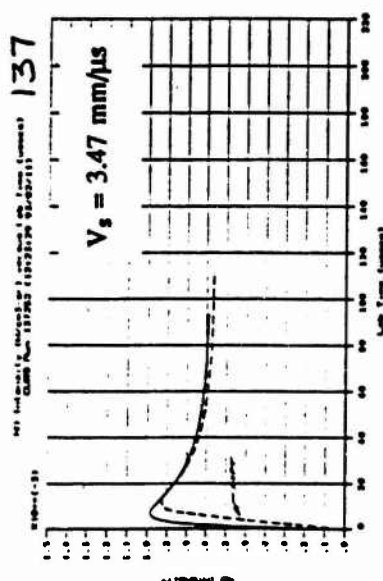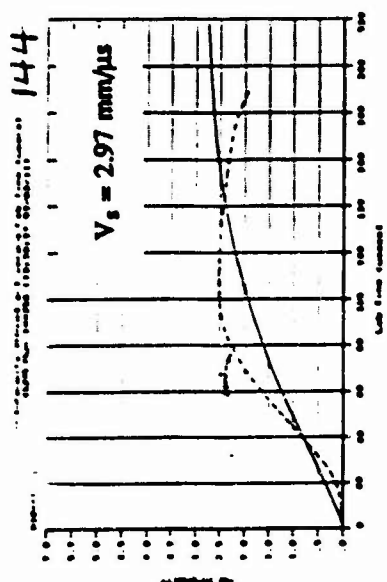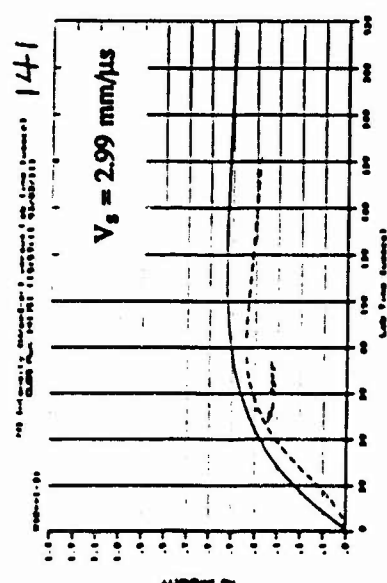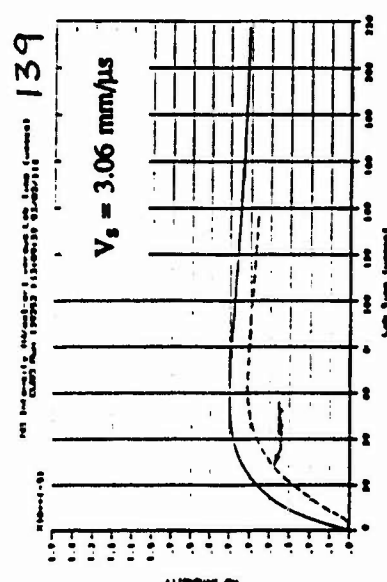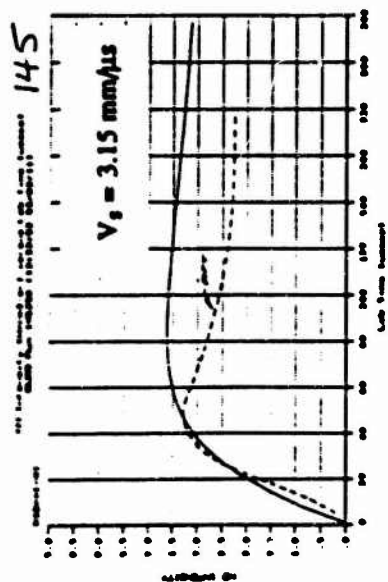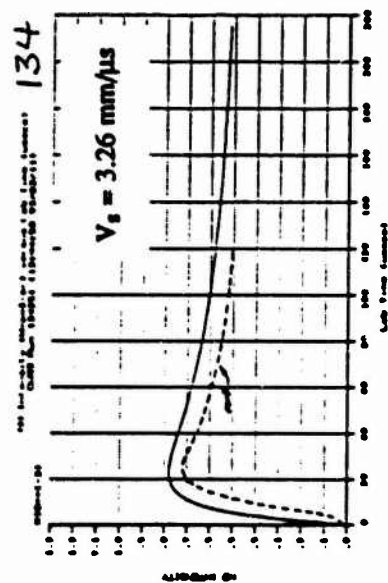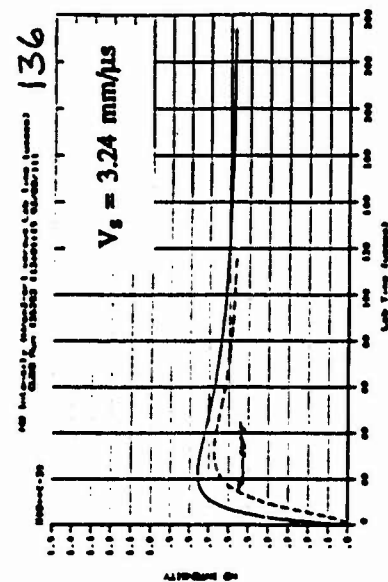
FIGURE 5. MEASURED AND CALCULATED 5.3 μm INTENSITY PROFILES

RATES FOR REACTIONS: 1,2,4-8,10   CAMAC (REF. 5)
                           3   JERIG (REF. 10), i.e. 0.47 TIMES CAMAC'S RATE
                           9   MONAT (REF. 9), i.e. 2.71 TIMES CAMAC'S RATE

(RUN NUMBER IN UPPER RIGHT CORNER OF EACH PLOT PROVIDES REFERENCE TO FULL-SCALE PROFILE IN APPENDIX A.)

21

Po = 2.25 torr

LAB TIME SCALE: 0 to 220 μs

40% O₂ / 60% N₂
INTENSITY SCALE: 0 to 1.5(-3) w/cm³-sr

135

Vₛ = 3.85 mm/μs

22.3% O₂ / 77.7 % N₂
INTENSITY SCALE: 0 to 13(-3) w/cm³-sr

132

Vₛ = 3.85 mm/μs

137

Vₛ = 3.47 mm/μs

133

Vₛ = 3.52 mm/μs

5% O₂ / 95% N₂
INTENSITY SCALE: 0 to 6.0 (-4) w/cm³-sr

147

Vₛ = 3.87 mm μs
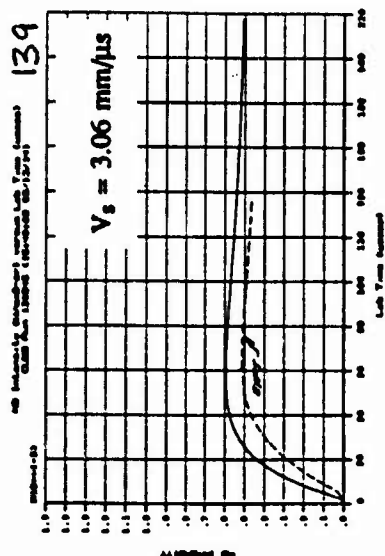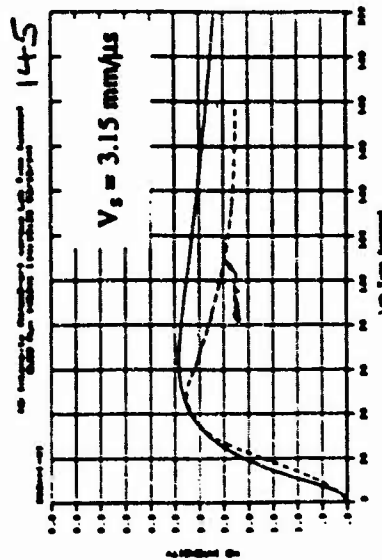
146

Vₛ = 3.49 mm/μs
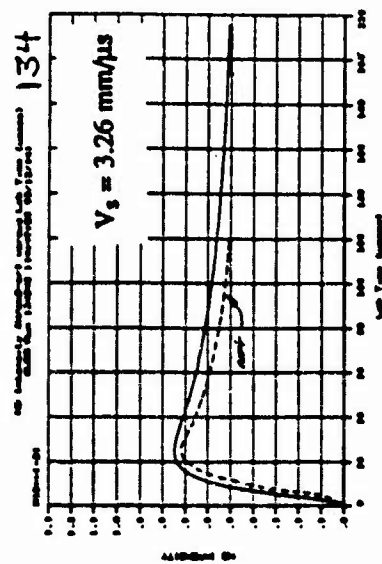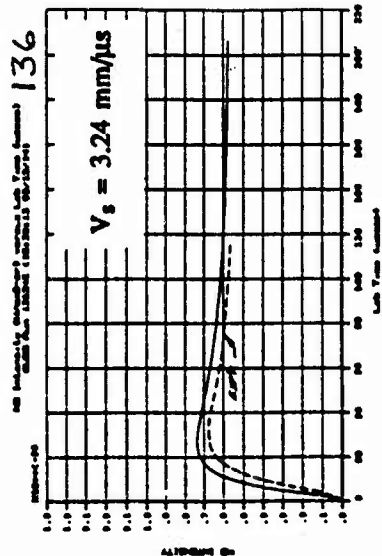
22
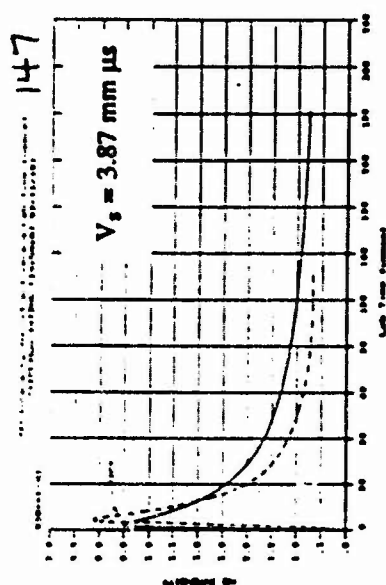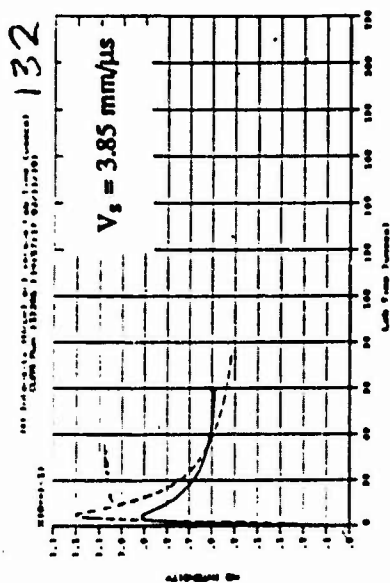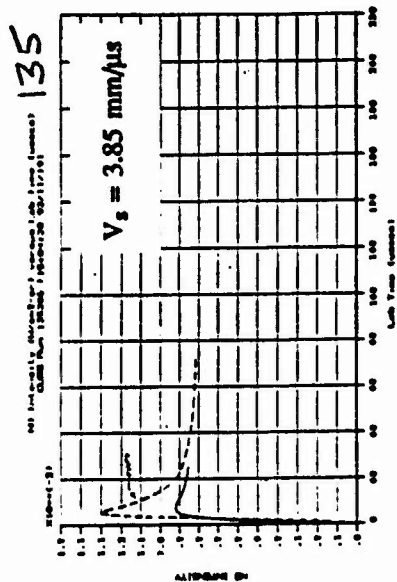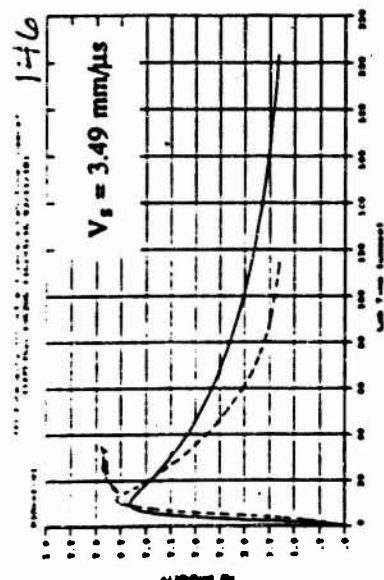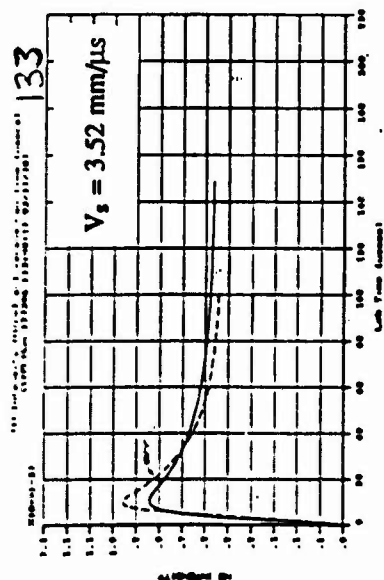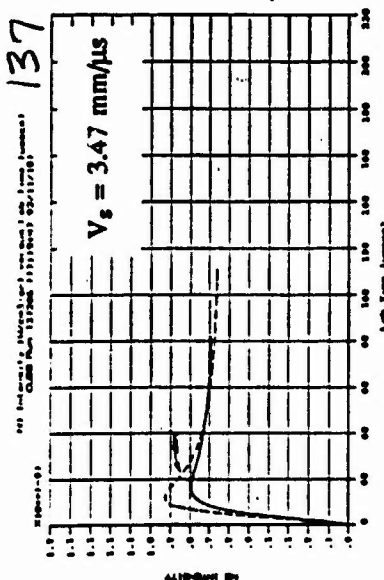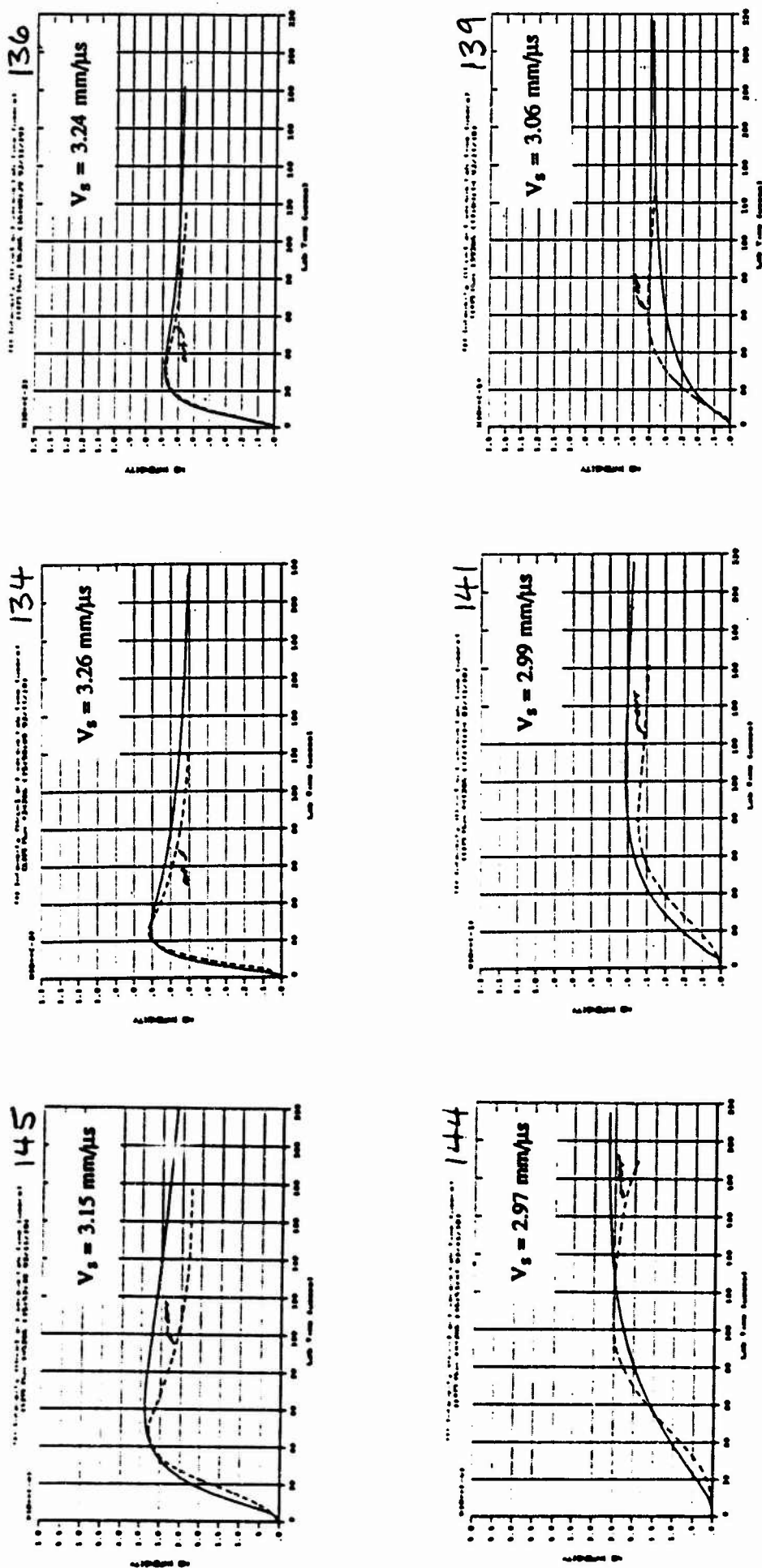
FIGURE 6. MEASURED AND CALCULATED 5.3 μm INTENSITY PROFILES

RATES FOR REACTIONS: 1-8,10   CAMAC (REF. 5)
                9   MONAT (REF. 9), i.e. 2.71 TIMES CAMAC'S RATE

VIBRATION-DISSOCIATION COUPLING PARAMETER, REACTION 9 ONLY: X=0.7

(RUN NUMBER IN UPPER RIGHT CORNER OF EACH PLOT PROVIDES REFERENCE TO FULL-SCALE PROFILE IN APPENDIX A.)

23

P₀ = 2.25 torr

LAB TIME SCALE: 0 to 220 µs

22.3% O₂ / 77.7 % N₂
INTENSITY SCALE: 0 to 1.3(-3) w/cm³-sr

40% O₂ / 60% N₂
INTENSITY SCALE: 0 to 1.5(-3) w/cm³-sr

5% O₂ / 95% N₂
INTENSITY SCALE: 0 to 6.0(-4) w/cm³-sr

V_s = 3.85 mm/µs   135

V_s = 3.47 mm/µs   137

V_s = 3.85 mm/µs   132

V_s = 3.52 mm/µs   133

V_s = 3.87 mm µs   147

V_s = 3.49 mm/µs   146

24
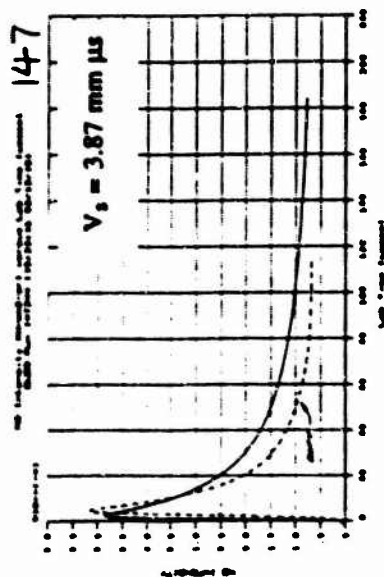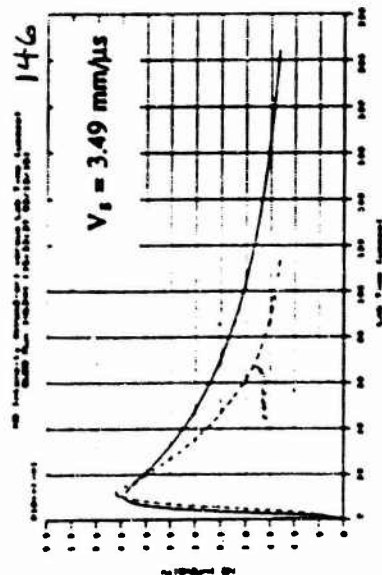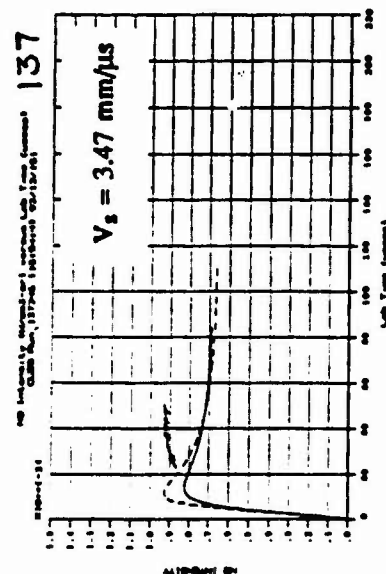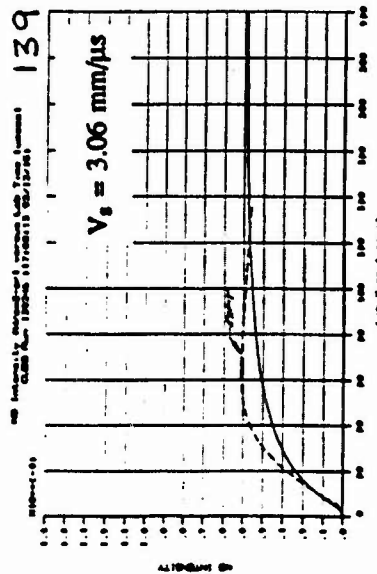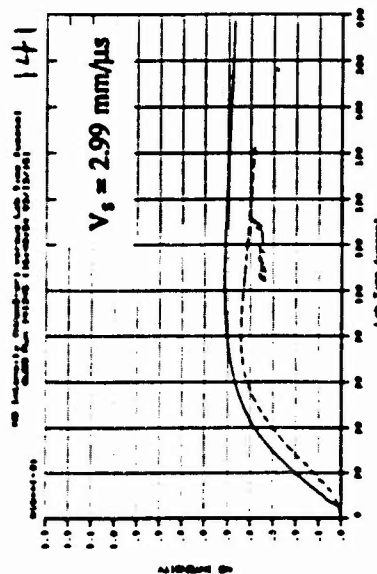
FIGURE 7. MEASURED AND CALCULATED 5.3 μm INTENSITY PROFILES

RATES FOR REACTIONS: 1-8,10   CAMAC (REF. 5)
                          9   MONAT (REF. 9), i.e. 2.71 TIMES CAMAC'S RATE

VIBRATION-DISSOCIATION COUPLING PARAMETER, REACTIONS 1-6,9: X=0.7

(RUN NUMBER IN UPPER RIGHT CORNER OF EACH PLOT PROVIDES REFERENCE TO FULL-SCALE PROFILE IN APPENDIX A.)

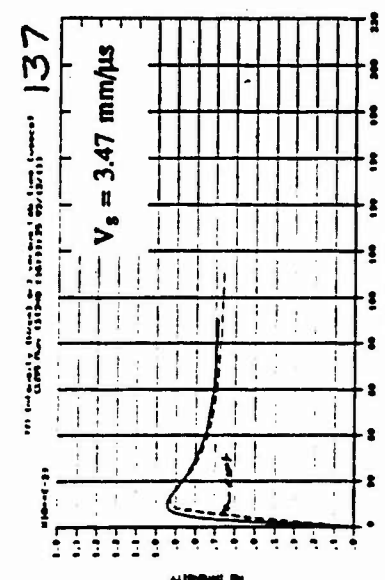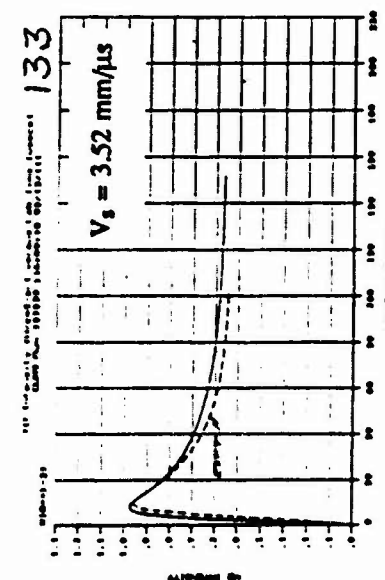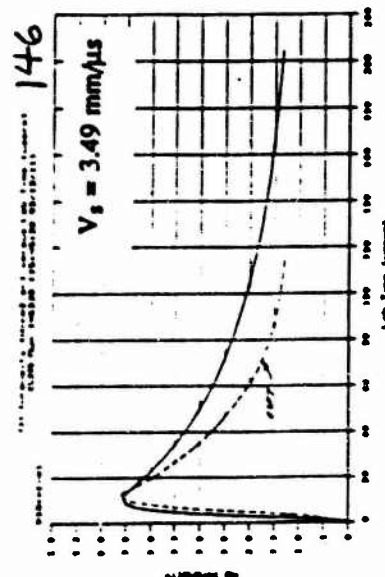25
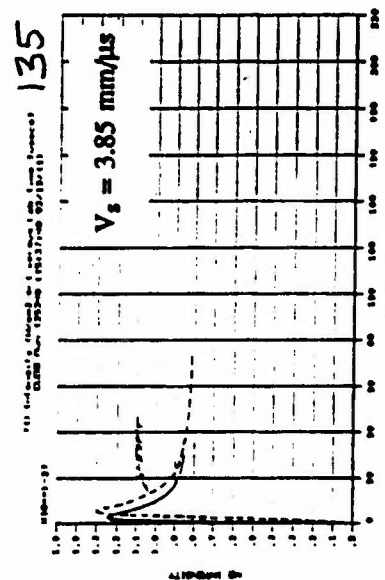
$P_0 = 2.25$ torr

LAB TIME SCALE: 0 to 220 µs

5% O$_2$/95% N$_2$
INTENSITY SCALE: 0 to 6.0 (-4) w/cm^3-sr

22.3% O$_2$/77.7 % N$_2$
INTENSITY SCALE: 0 to 1.3(-3) w/cm^3-sr

40% O$_2$/60% N$_2$
INTENSITY SCALE: 0 to 1.5(-3) w/cm^3-sr

147

$V_s = 3.87$ mm µs

132

$V_s = 3.85$ mm/µs

135

$V_s = 3.85$ mm/µs

146

$V_s = 3.49$ mm/µs

133

$V_s = 3.52$ mm/µs

137

$V_s = 3.47$ mm/µs

26
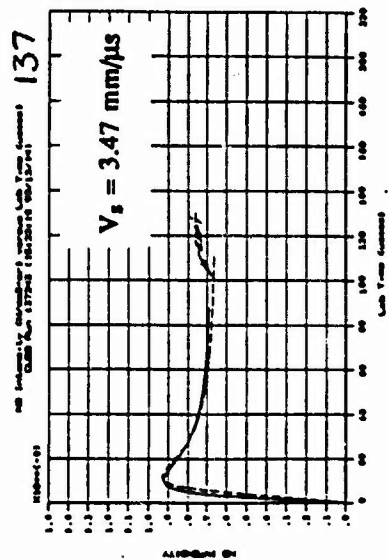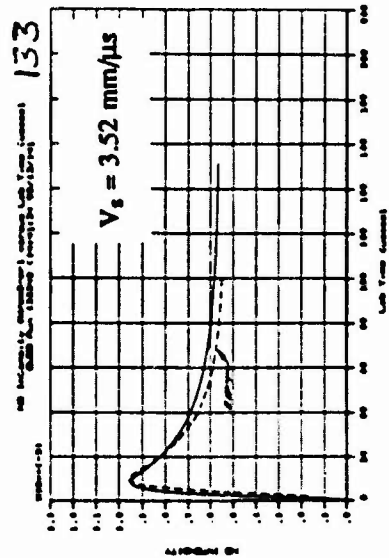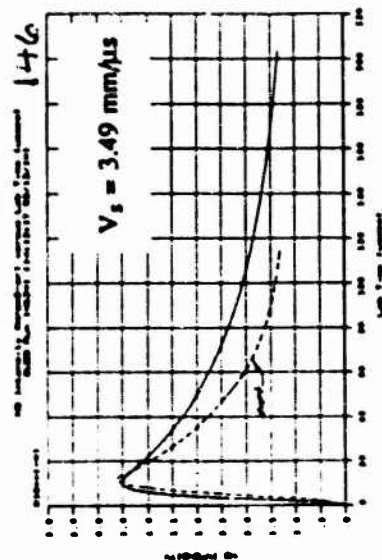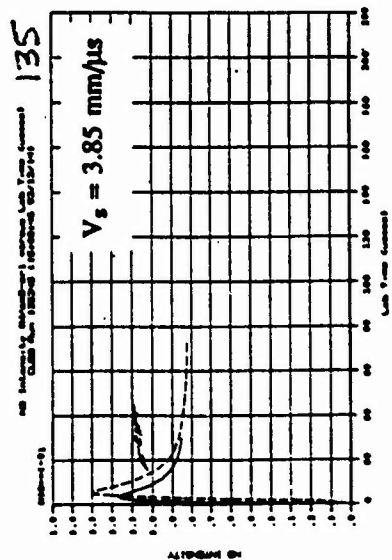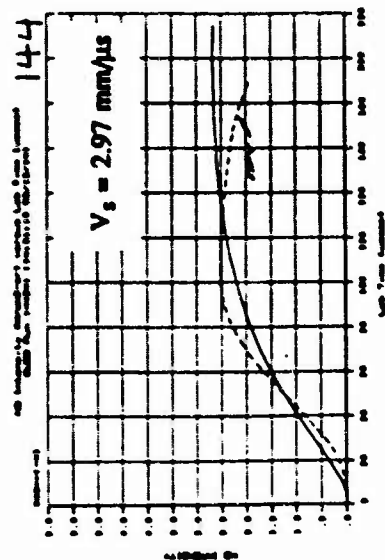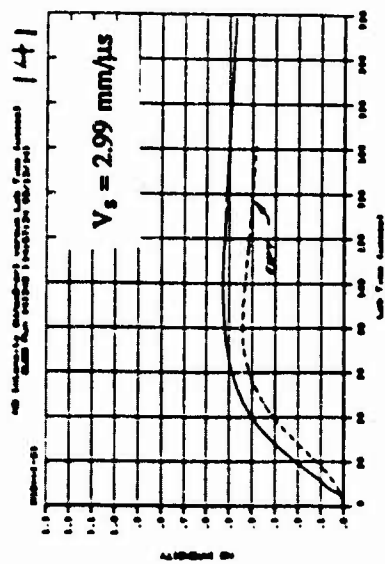
FIGURE 8. MEASURED AND CALCULATED 5.3 μm INTENSITY PROFILES

RATES FOR REACTIONS: 1-8,10   CAMAC (REF. 5)
                              9   MONAT (REF. 9), i.e. 2.71 TIMES CAMAC'S RATE

VIBRATION-DISSOCIATION COUPLING PARAMETER, REACTIONS 1-6,9: X=0.7
N₂ VIBRATIONAL RELAXATION TIME ADJUSTMENT PARAMETER: P=0.3

(RUN NUMBER IN UPPER RIGHT CORNER OF EACH PLOT PROVIDES REFERENCE TO FULL-SCALE PROFILE IN APPENDIX A.)

27

5% O_2 / 95% N_2
INTENSITY SCALE: 0 to 6.0(-4) w/cm³-sr

22.3% O_2 / 77.7 % N_2
INTENSITY SCALE: 0 to 1.3(-3) w/cm³-sr

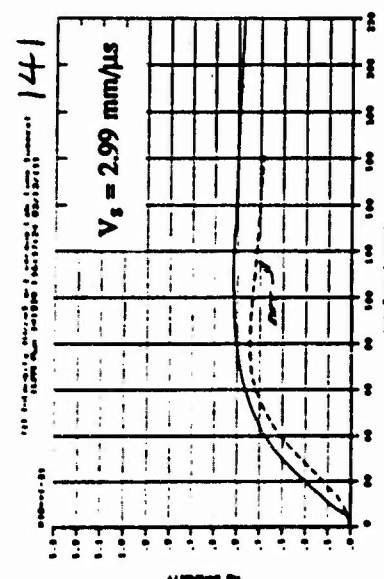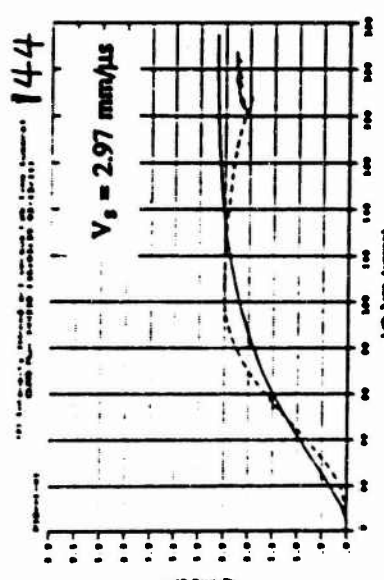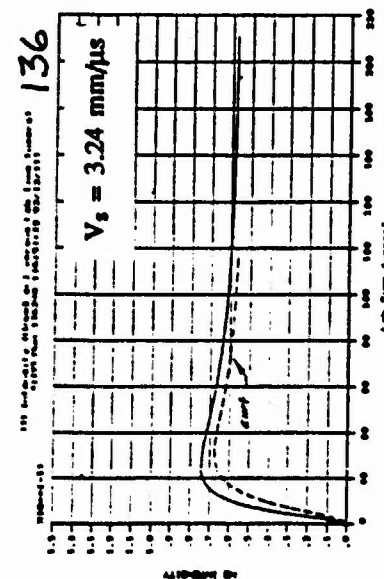40% O_2 / 60% N_2
INTENSITY SCALE: 0 to 1.5(-3) w/cm³-sr

147

$V_s = 3.87$ mm μs

132

$V_s = 3.85$ mm/μs

135

$V_s = 3.85$ mm/μs

146

$V_s = 3.49$ mm/μs

133

$V_s = 3.52$ mm/μs

137

$V_s = 3.47$ mm/μs
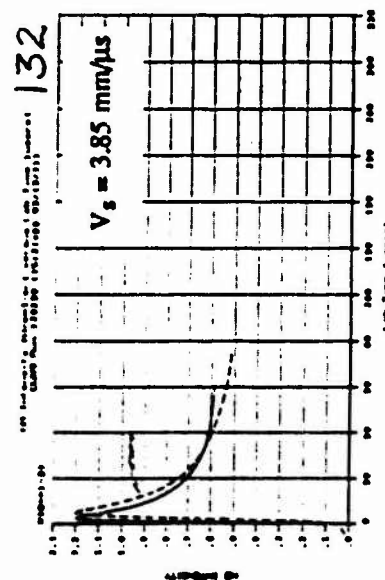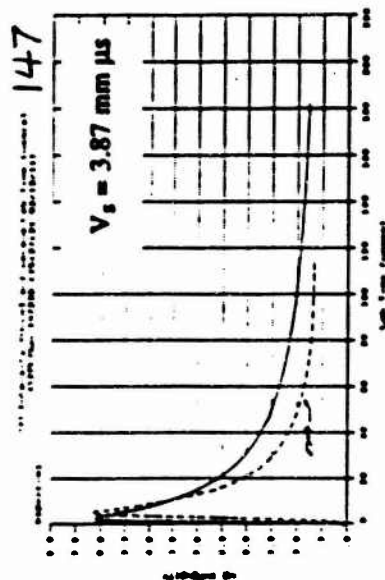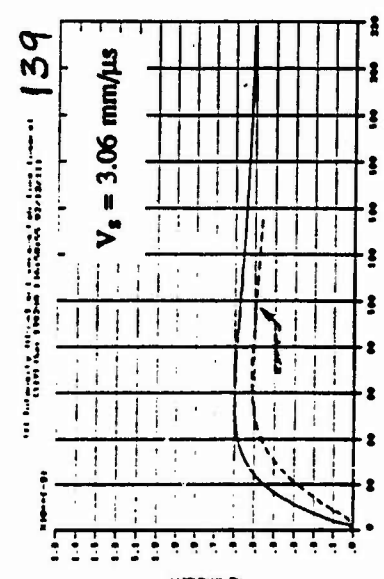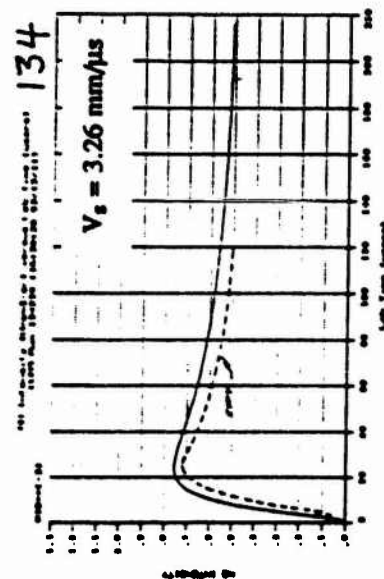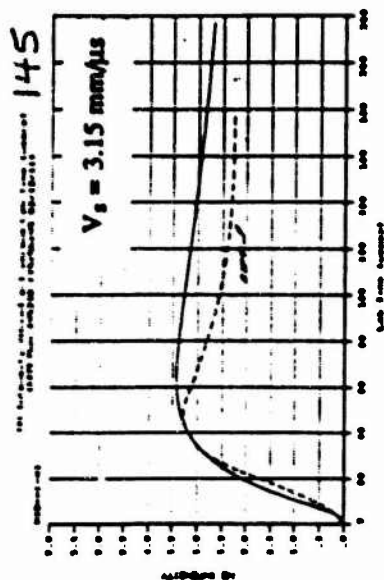
FIGURE 9. MEASURED AND CALCULATED 5.3 μm INTENSITY PROFILES

RATES FOR REACTIONS: 1-8,10   CAMAC (REF. 5)
             9   MONAT (REF. 9), i.e. 2.71 TIMES CAMAC'S RATE

VIBRATION-DISSOCIATION COUPLING PARAMETER, REACTIONS 1-6,9: X=0.7
N_2 VIBRATIONAL RELAXATION TIME ADJUSTMENT PARAMETER: P=0.2

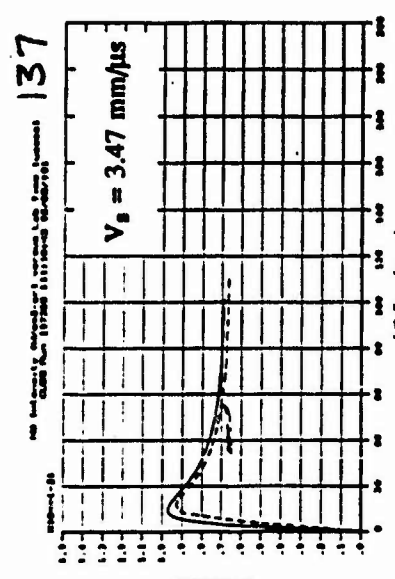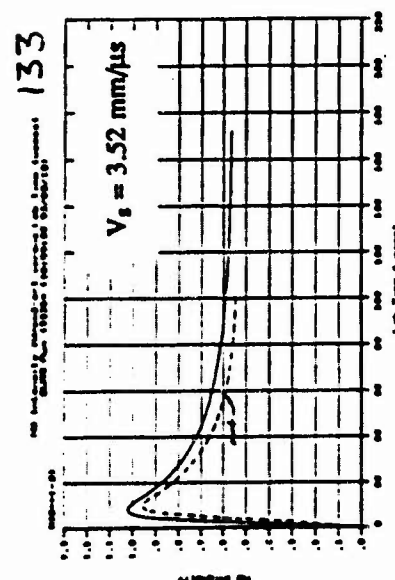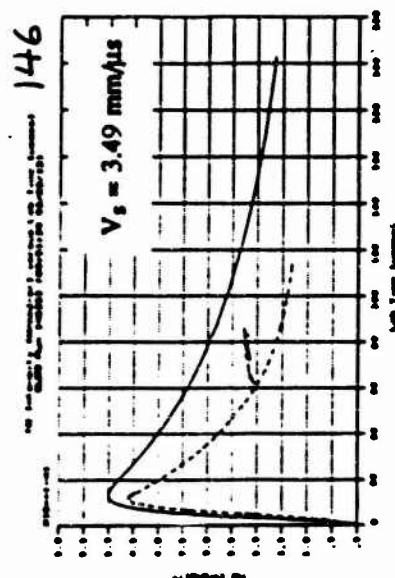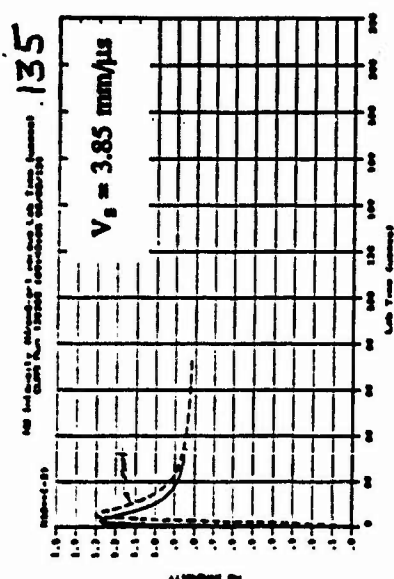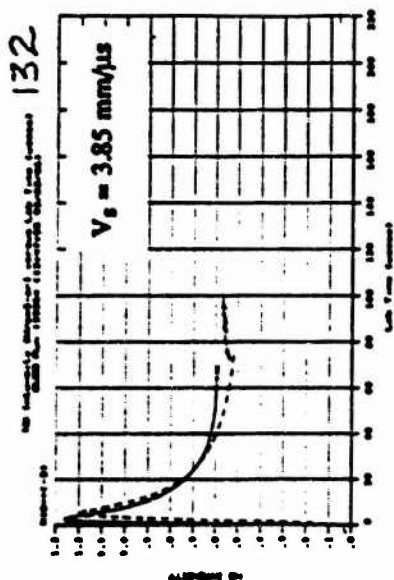(RUN NUMBER IN UPPER RIGHT CORNER OF EACH PLOT PROVIDES REFERENCE TO FULL-SCALE PROFILE IN APPENDIX A.)
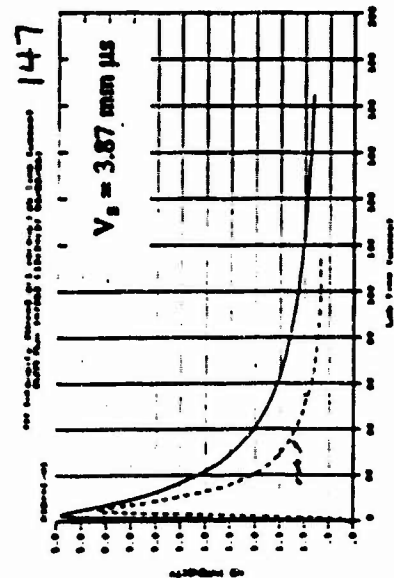
FIGURE 10. MEASURED AND CALCULATED 5.3 µm INTENSITY PROFILES

RATES FOR REACTIONS: 1-8,10   CAMAC (REF. 5)
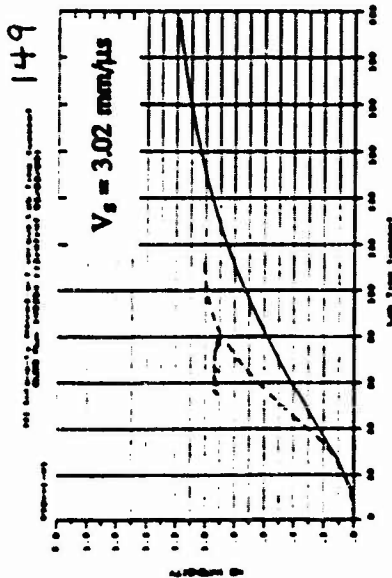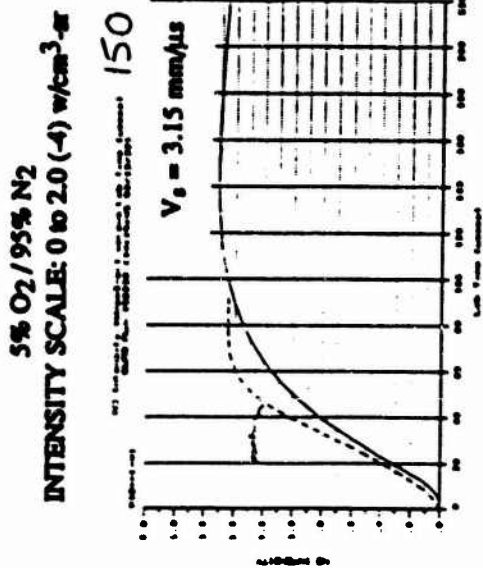   3   JERIG (REF. 10), i.e., 0.47 TIMES CAMAC'S RATE
               9   MONAT (REF. 9), i.e. 2.71 TIMES CAMAC'S RATE

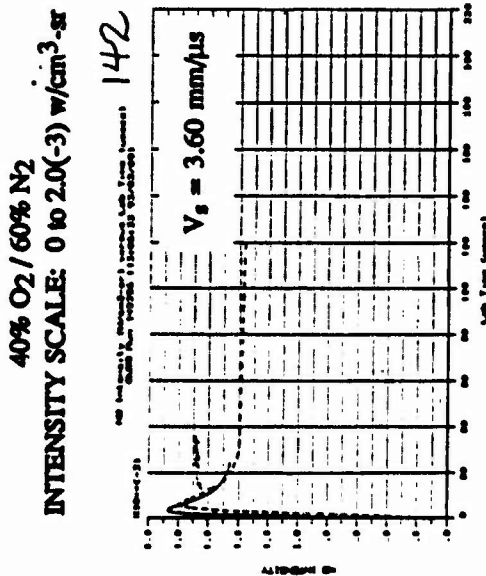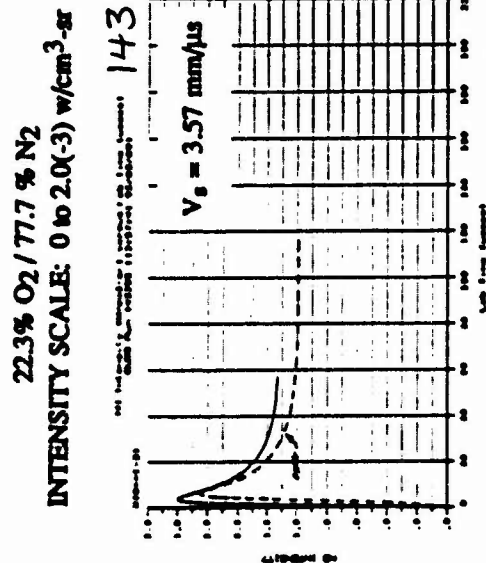VIBRATION-DISSOCIATION COUPLING PARAMETER, REACTIONS 1-6,9: X=0.7
N_2 VIBRATIONAL RELAXATION TIME ADJUSTMENT PARAMETER: P=0.2

(RUN NUMBER IN UPPER RIGHT CORNER OF EACH PLOT PROVIDES REFERENCE TO FULL-SCALE PROFILE IN APPENDIX A.)

LAB TIME SCALE: 0 to 220 μs

40% O₂ / 60% N₂
INTENSITY SCALE: 0 to 2.0(-3) w/cm³-sr   142

V$_s$ = 3.60 mm/μs

22.3% O₂ / 77.7 % N₂
INTENSITY SCALE: 0 to 2.0(-3) w/cm³-sr   143

V$_s$ = 3.57 mm/μs

P$_0$ = 4.00 torr

5% O₂ / 95% N₂
INTENSITY SCALE: 0 to 2.0 (-4) w/cm³-sr   150

V$_s$ = 3.15 mm/μs

V$_s$ = 3.02 mm/μs   149
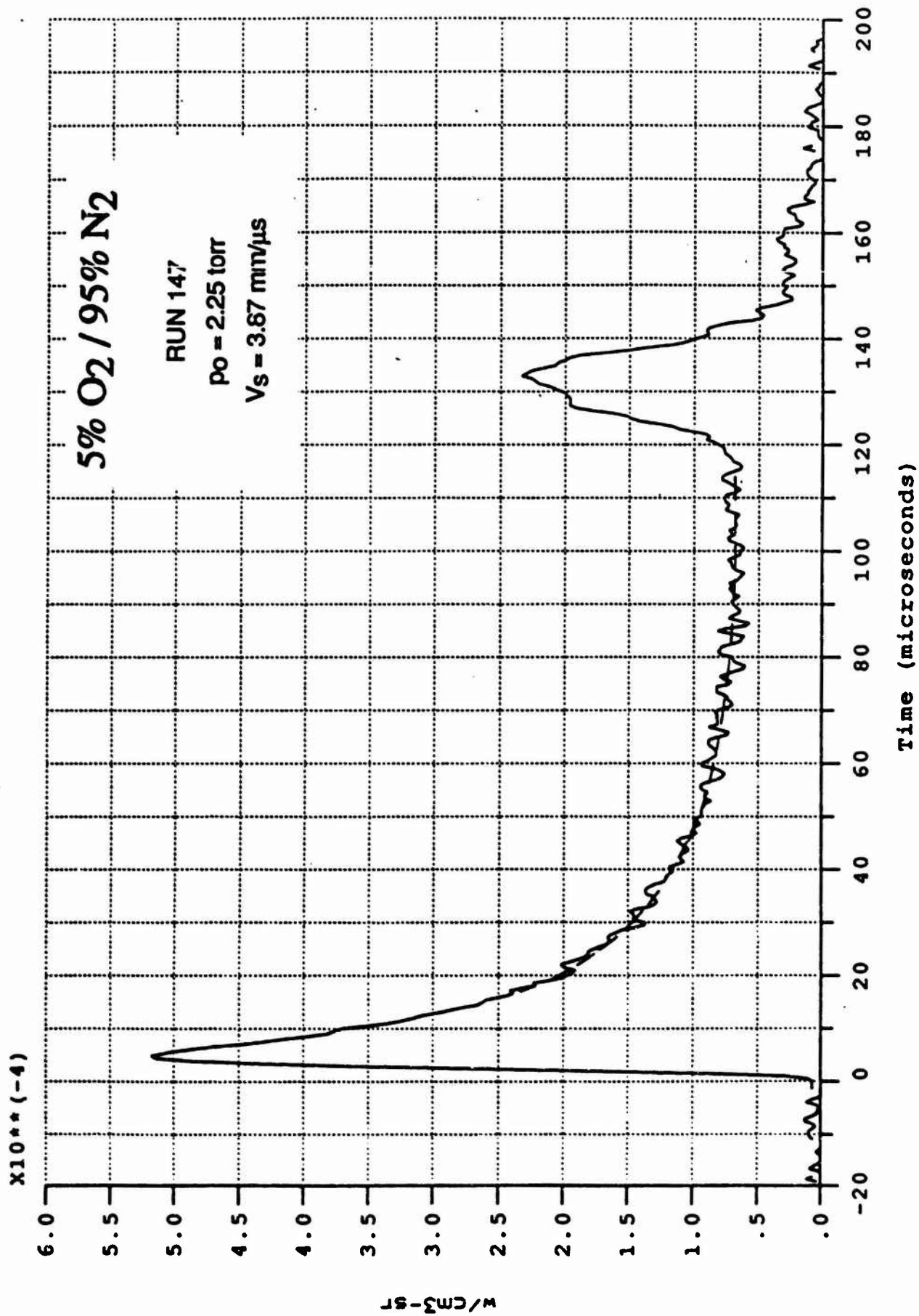
P$_0$ = 1.00 torr

FIGURE 11. MEASURED AND CALCULATED 5.3 μm INTENSITY PROFILES

RATES FOR REACTIONS: 1-8,10   CAMAC (REF. 5)
                              9   MONAT (REF. 9), i.e. 2.71 TIMES CAMAC'S RATE
VIBRATION-DISSOCIATION COUPLING PARAMETER, REACTIONS 1-6,9: X=0.7
N₂ VIBRATIONAL RELAXATION TIME ADJUSTMENT PARAMETER: P=0.2

(RUN NUMBER IN UPPER RIGHT CORNER OF EACH PLOT PROVIDES REFERENCE TO FULL-SCALE PROFILE IN APPENDIX A.)

31

APPENDIX A

Full-Scale Experimental Intensity Profiles

5% O₂ / 95% N₂

RUN 147
po = 2.25 torr
Vs = 3.67 mm/μs

x10**(-4)

w/CM3-sr

Time (microseconds)

5% O_2 / 95% N_2

RUN 146
Po = 2.25 torr
Vs = 3.49 mm/µs

X10**(-4)

W/CM3-SR

Time (microseconds)

5% O₂ / 95% N₂

RUN 145
po = 2.25 torr
Vs = 3.15 mm/µs

X10**(-4)

Time (microseconds)

W/CM3-SL

A-4

5% O₂ / 95% N₂

RUN 144

po = 2.25 torr

Vs = 2.97 mm/µs

A-5

22.3% O₂ / 77.7 % N₂

RUN 132
po = 2.25 torr
Vs = 3.85 mm/µs

X10** (-3)

W/CM3-SR

Time (microseconds)

A-6

22.3% O₂ / 77.7 % N2

RUN 133
po = 2.25 torr
Vs = 3.52 mm/μs

X10**(-3)

W/CM3-SR

Time (microseconds)

A-7

22.3% O2 / 77.7 % N2

RUN 134
po = 2.25 torr
Vs = 3.26 mm/μs

X10**(-3)

W/CM3-SR

Time (microseconds)

A-8

X10**(-3)

22.3% O_2 / 77.7 % N_2

RUN 141

$p_0 = 2.25$ torr

$V_s = 2.99$ mm/μs

w/CM3-sr

Time (microseconds)

X10**(-3)

40% O2 / 60% N2

RUN 135
po = 2.25 torr
Vs = 3.85 mm/μs

W/CM3-sr

Time (microseconds)

A-10

X10**(-3)

40% O2 / 60% N2

RUN 137
po = 2.25 torr
Vs = 3.47 mm/μs

w/CM3-sr

Time (microseconds)

A-11

40% O₂ / 60% N₂

RUN 136

po = 2.25 torr

Vs = 3.24 mm/µs

X10**(-3)

W/CM3-sr

Time (microseconds)

A-12

40% O$_2$ / 60% N$_2$

RUN 139

p$_o$ = 2.25 torr

V$_s$ = 3.06 mm/µs

X10**(-3)

W/CM3-sr

Time (microseconds)

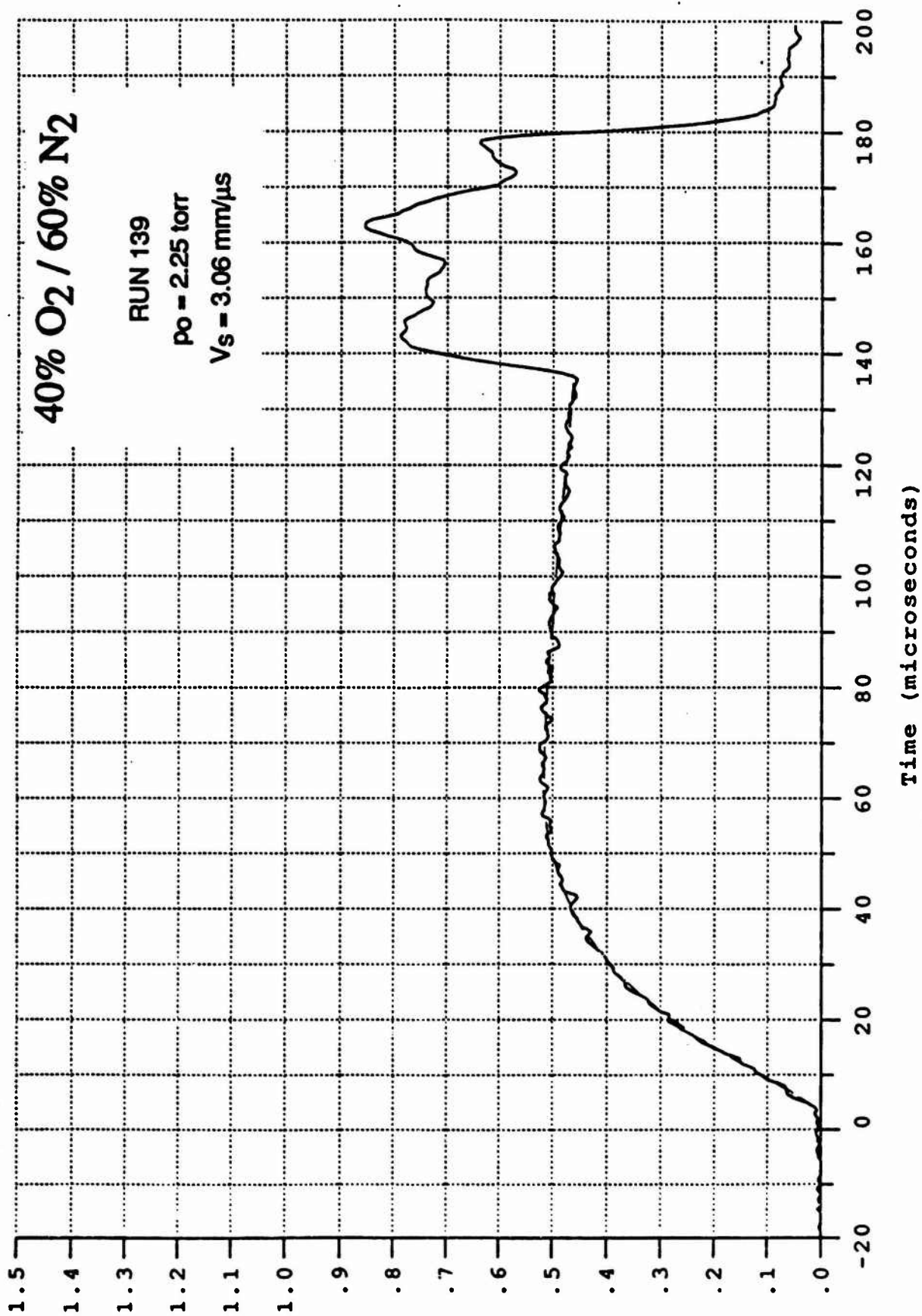A-13

5% O₂ / 95% N₂

RUN 150

po = 1.00 torr

Vs = 3.15 mm/μs

X10**(-4)

W/CM3-SR

Time (microseconds)

A-14

X10**(-4)

5% O₂ / 95% N₂ → $5\% \ O_2 \ / \ 95\% \ N_2$

RUN 149

po = 1.00 torr → $p_o = 1.00 \ torr$

Vs = 3.02 mm/μs → $V_s = 3.02 \ mm/\mu s$

Time (microseconds)

W/CM3-SF

A-15

RUN 143

po = 4.00 torr

Vs = 3.57 mm/μs

22.3% O2 / 77.7 % N2

X10**(−3)

W/CM3-SR

Time (microseconds)

A-16

X10**(-3)

40% O2 / 60% N2

RUN 142
po = 4.00 torr
Vs = 3.60 mm/μs

W/CM3-sr

Time (microseconds)

A-17